

# PREPARATION AND DIELECTRIC MEASUREMENTS OF NIOBIUM PENTAOXIDE DOPED BARIUM STRONTIUM TITANATE GLASS AND GLASS CERAMICS




Final Year B-Tech thesis  
submitted by  
**Bijay Kumar Barkey**

under the guidance of  
**Prof. Partha Saha**

## Certificate

This is to certify that the work presented in this thesis entitled as “**Preparation and Dielectric Measurements of Niobium Pentoxide doped Barium Strontium Titanate Glass and Glass Ceramics**” by Bijay Kumar Barkey, roll number 111CR0092, is an original research work which is completed by him under my guidance to complete his course and achieve his B-Tech degree in Ceramic Engineering National Institute of Technology, Rourkela.



**Prof. Partha Saha**  
Department of Ceramic Engineering  
National Institute of Technology, Rourkela

## Acknowledgement

I express my deep sense of gratitude to all the peoples without whom I would never had completed my project. I would really like to say thanks to my supervisor, Prof. Partha Saha, Department of Ceramic Engineering, National Institute of Technology Rourkela, for his strategic efforts for helping me complete the project. I am very much thankful to all the professors of Department of Ceramic Engineering, NIT Rourkela, who helped me with every fundamental details about my project that altogether profited me in successfully completing my work. I would also like to express my profound gratitude to all the staff members of National Institute of Technology, Rourkela for helping me during the experimental work as and when required.

I take this opportunity to express profound gratitude to my friends and associates who have given their support each time I required. The commitments bestowed by them was without a doubt a major boost to achieve my goals. At last, I truly want to express profound gratitude to my parents, who have been a constant inspiration and motivation to do well and achieve greater heights in life.

A handwritten signature in black ink, reading "Bijay Kumar Barik". The signature is written in a cursive style with a large, looping 'B' at the beginning and a long, sweeping tail at the end.

## ABSTRACT

(Ba<sub>0.2</sub>Sr<sub>0.8</sub>)TiO<sub>3</sub>-B<sub>2</sub>O<sub>3</sub>-K<sub>2</sub>O based glass as well as glass ceramic with and without 0.1 mol % Nb<sub>2</sub>O<sub>5</sub> were developed by the conventional melt quench method. XRD and FTIR spectra of the glass samples confirms the formation of amorphous structure and presence of stretching and deformation vibrations of B-O-Si linkage and Si-O-Si bridges, respectively. Differential scanning calorimetry (DSC) of the glass sample reveals that addition of 0.1 mol % Nb<sub>2</sub>O<sub>5</sub> elevates the onset of crystallization temperature from ~600°C to ~675°C. XRD reveals that desired SrBaTiO<sub>3</sub> phase was formed upon controlled crystallization of the glass samples at ~750-780°C for 3h. SEM-EDS analysis of the un-doped glass ceramic sample shows the formation of micron sized flower-like, and needle shaped crystals. However addition of 0.1 mol % Nb<sub>2</sub>O<sub>5</sub> modifies the microstructure to irregular shaped crystals. Results from the dielectric measurements suggest that upon addition of 0.1 mol % Nb<sub>2</sub>O<sub>5</sub> the dielectric constant remains the same as compared to the un-doped sample.

**KEYWORDS:** Glass, Glass Ceramic, perovskite, Paraelectric, Dielectric measurement

## CONTENTS

LIST OF TABLES.....	6
LIST OF FIGURES .....	7-8
1 INTRODUCTION .....	9
1.1 PEROVSKITE STRUCTURE .....	9-10
2 LITERATURE RIVIEW .....	10-17
3 EXPERIMENTAL PROCEDURE .....	17-20
3.1 MATERIALS .....	17
3.2 GLASS PREPARATION .....	17-18
3.3 INFRARED SPECTROSCOPY .....	18
3.4 DIFFERENTIAL SCANNING CALORIMETRY STUDY.....	18
3.5 DENSITY MEASUREMENT .....	18-19
3.6 GLASS CERAMIC PREPARATION .....	19
3.7 IDENTIFICATION OF CRYSTALLINE PHASES.....	19
3.8 MICROSTRUCTURAL STUDIES.....	19-20
3.9 DIELECTRIC MEASUREMENT .....	20
4 RESUL AND DISCUSSION .....	20-41
4.1 XRD ANALYSIS OF GLASS.....	20-23
4.2 INFRARED SPECTROSCOPY ANALYSIS.....	23-25
4.3 (DSC) ANALYSIS .....	25-27
4.4 DENSITY ANALYSIS .....	27-28
4.5 XRD ANALYSIS OF GLASS CERAMIC.....	29-31
4.6 SEM ANALYSIS .....	31-36
4.7 DIELECTRIC ANALYSIS .....	36-41
5 CONCLUSION .....	41-42
6 REFERENCES .....	43-44

## LIST OF TABLES

<b>Sl. No.</b>	<b>Table</b>	<b>Page no</b>
<b>Table 1</b>	Density study for Glass Samples	28
<b>Table 2</b>	Density study for Glass Ceramic samples	29

## LIST OF FIGURES

Sl. No.	Figure	Page No
<b>Fig. 1</b>	Perovskite structure centered around Ti ion	10
<b>Fig. 2</b>	XRD pattern of $[(Ba_{0.2}Sr_{0.8})O.TiO_2]-[2SiO_2-B_2O_3]-[K_2O]$ glass quenched on a preheated graphite plate	22
<b>Fig. 3</b>	XRD pattern of $[(Ba_{0.2}Sr_{0.8})O.TiO_2]-[2SiO_2-B_2O_3]-[K_2O]$ glass quenched at room temperature	22
<b>Fig. 4</b>	XRD pattern of $[(Ba_{0.2}Sr_{0.8})O.TiO_2]-[2SiO_2-B_2O_3]-[K_2O]$ 0.1 mol % $[Nb_2O_5]$ glass quenched at room temperature	23
<b>Fig. 5</b>	FTIR spectra of SBT base glass	24
<b>Fig. 6</b>	FTIR spectra of 0.1 mol % $Nb_2O_5$ doped SBT glass	25
<b>Fig. 7</b>	DSC scan from room temperature to 800 °C of base glass quenched on preheated graphite plate	26
<b>Fig. 8</b>	DSC study of from room temperature to 700 °C of air quenched base glass sample	27
<b>Fig. 9</b>	DSC study from room temperature to 700 °C of 0.1 mol % $Nb_2O_5$ doped glass sample	27
<b>Fig. 10</b>	XRD pattern of $[(Ba_{0.2}Sr_{0.8})O.TiO_2]-[2SiO_2-B_2O_3]-[K_2O]$ glass sample quenched on a preheated graphite plate and then crystallized at 750°C as well as at 780°C for 3h in air	30
<b>Fig. 11</b>	XRD pattern of $[(Ba_{0.2}Sr_{0.8})O.TiO_2]-[2SiO_2-B_2O_3]-[K_2O]$ glass sample quenched at room temperature and then crystallized at 750°C as well as at 780°C for 3h in air	31
<b>Fig. 12</b>	XRD pattern of $[(Ba_{0.2}Sr_{0.8})O.TiO_2]-[2SiO_2-B_2O_3]-[K_2O]-0.1$ mol % $[Nb_2O_5]$ glass sample quenched at room temperature and then crystallized at 750°C for 3h in air	31
<b>Fig. 13</b>	SEM images of SBT base glass ceramic	33
<b>Fig. 14</b>	EDS analysis of flower like crystal found in the microstructure	33
<b>Fig. 15</b>	EDS analysis of needle like crystal found in the base glass ceramic	33
<b>Fig. 16</b>	EDS analysis of the matrix phase of base glass ceramic	34
<b>Fig. 17</b>	EDS analysis of dendritic microstructure	34
<b>Fig. 18</b>	Elemental X-ray mapping showing the distributioun of elements from SBT base glass ceramic	34
<b>Fig. 19</b>	SEM image of 0.1mol % $Nb_2O_5$ doped glass ceramic	35
<b>Fig. 20</b>	EDS analysis for irregular shaped crystals in the microstructure	35
<b>Fig. 21</b>	EDS analysis of the matrix phase for doped glass ceramic	35
<b>Fig. 22</b>	Elemental X-ray mapping showing the distributioun of elements for 0.1 mol % doped $Nb_2O_5$ SBT glass ceramic	36
<b>Fig. 23</b>	Dielectric measurement of SBT base glass ceramics at room temperature	38
<b>Fig. 24</b>	Dielectric measurement of doped glass ceramics at room temperature	39
<b>Fig. 25</b>	Measurement of dielectric constant with varying temperature for SBT base glass ceramic	39

<b>Fig. 26</b>	Measurement of dissipation factor with varying temperature for SBT base glass ceramic	40
<b>Fig. 27</b>	Measurement of dielectric constant with varying temperature for 0.1 mol % Nb <sub>2</sub> O <sub>5</sub> doped SBT glass ceramic	40
<b>Fig. 28</b>	Measurement of dissipation factor with varying temperature for 0.1 mol % Nb <sub>2</sub> O <sub>5</sub> doped SBT glass ceramic	41



## **1. INTRODUCTION**

Glass ceramic were discovered somewhat accidently in 1953, since then a number of patents and papers have been published by academic institutes and companies worldwide. Polycrystalline material or glass ceramics are formed when a particular composition of glass is taken at an elevated temperature and thereby heat treated as a result controlled crystallization of the glass sample takes place. It is observed that formation of glass ceramic is only possible if some nucleating agent or additive is present in the composition. However, some glasses are difficult to crystallize as they are very stable, *viz.*, common soda-lime-silica glass. Whereas few glasses readily undergo crystallization resulting in formation of glass ceramics. The glass ceramic shows dual properties like it can easily be fabricated using melt quench method and possess the properties of glass as well as show high compressive strength observed in ceramics. Glass ceramic are never fully crystalline, the crystalline phase are in the range of 50 – 90 vol. % and the rest is glassy phase. The composition of the crystalline phase are normally different from that of the initial glass composition.

Glass ceramics have got many advantages such as high strength, toughness, high density, translucency, opacity, and low thermal expansion, stability at high temperature, ferromagnetism, bioactivity, biocompatibility, and high chemical durability. The glass ceramic manufacturing technique involves the preparation of glass using the conventional melt quench method and then the glass sample is subjected suitable heat treatment in a furnace to transform in to glass ceramic. During this heat treatment desired crystalline phases are precipitated in to the glassy matrix, and it is seen that some nucleating agents present in the base glass control the crystallization process.

### **1.1 PEROVSKITE STRUCTURE**

Perovskite structure are found in materials which have a crystal structure similar to that of the calcium titanate ( $\text{CaTiO}_3$ ). It got its name from a mineral which was found in the Ural

Mountains, Russia and was named after. L.A. Perovski- a Russian mineralogist. The general formula of perovskite structure is  $ABX_3$  in which A and B denotes cations with dissimilar sizes and X forms bonds with both 'A' and 'B' cations. Crystallographic symmetry of the structure is cubic with 'A' cation having coordination number 12 whereas 'B' cation has 6.

In order to achieve a stable cubic structure the relative ionic radii must be perfect because slight deviation may lead to distortion in the crystal structure which can create several low-symmetry distorted version. Due to these distortions in the structure the coordination number of 'A' cation decreases which allows the 'B' cation to take a stable bonding pattern. Hence the dipoles resulting from these distortions are responsible for the ferroelectric behaviour which is shown by perovskites such as  $BaTiO_3$ . [1]

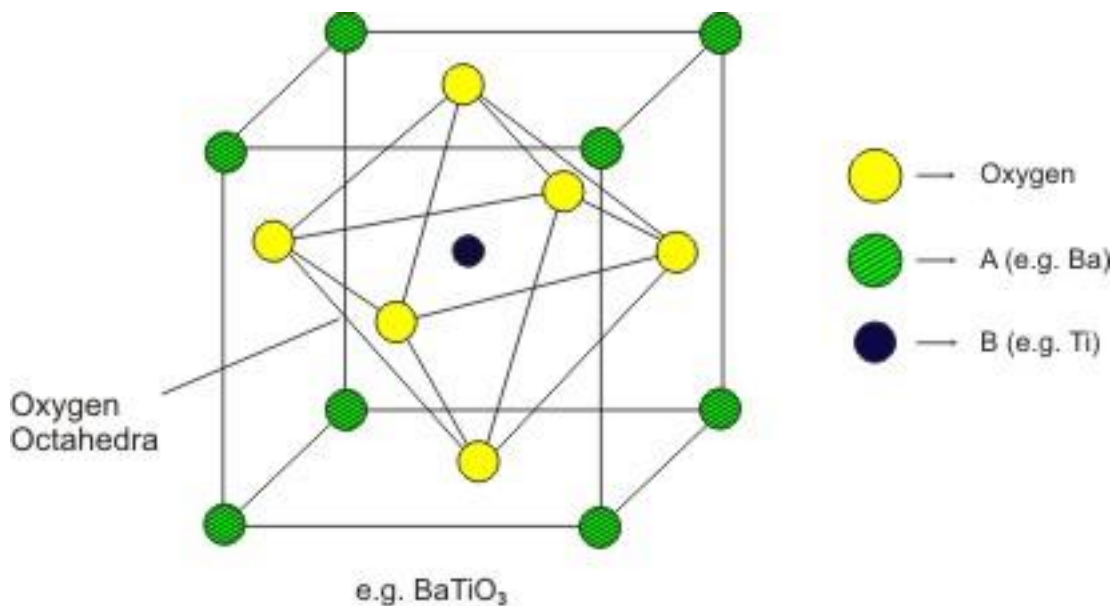


**Fig. 1** Perovskite structure centered around Ti ion

## 2. LITERATURE RIVIEW

A K Yadav *et al.* [2] studied the dielectric behaviour of lanthanum added barium strontium Titanate (BST) glass ceramic and deduced the following observations. In glass ceramic when  $Ba^{2+}$  is substituted in place of  $Sr^{2+}$  it leads to an increase in ionic conductivity with increase in frequency and thereby increases conductivity in various glass ceramics phases which is responsible for the enhancement of the dielectric constant. The borosilicate glass

former present in BST promotes crystallization at lower sintering temperature and when compared the energy density of pure BST ceramics and BST glass ceramic it is found that it increases up to 8.5 times than that of the pure BST ceramics. It is also observed that the energy density of the BST glass ceramic increased up to 2.56 times due to the addition of  $\text{La}_2\text{O}_3$ , moreover it plays a major role modifying the tetragonality of the barium strontium phase as it is diffused into the lattice structure. For the ease of formation of BST glass ceramic they observed that mainly borosilicate or aluminosilicate network forming systems accompanying some nucleating agents like  $\text{CeO}_2$ ,  $\text{Fe}_2\text{O}_3$  and  $\text{Nb}_2\text{O}_5$ , are favourable for the preparation of BST glass ceramic, and these oxides help to enhance the dielectric properties like increasing the dielectric constant with low dielectric loss. According to the XRD patterns it is seen that the glasses are crystallized to the major crystalline phase as BST and in addition to some pyrochlore phase ( $\text{BaTi}_2\text{Si}_2\text{O}_8$ ) are also evident. It was also observed that the un-doped glass ceramic has 19 volume percent secondary phase whereas in the doped glass ceramic it was 16 percent. Hence the author's concluded that the addition of  $\text{La}_2\text{O}_3$  doping enhances the crystallization of BST by decreasing the amount of the secondary phase. This addition of 1 mol. % of  $\text{La}_2\text{O}_3$  decreases the crystallite size, also promotes crystallization and the degree of crystallinity and also it acts as an nucleating agent which controls the nucleation and crystallization of BST borosilicate glass ceramics. The perovskite structure becomes more stable upon substitution of  $\text{La}^{3+}$  into  $\text{Ba}^{2+}$  sites because of the higher bond strength of La-O as compared to Ba-O bonds as a result suppresses the formation of intrinsic defects due to stronger chemical bonds. Through the results of the scanning electron micrographs it was found that addition of 1 mol. %  $\text{La}_2\text{O}_3$  plays an important role during nucleation and growth of crystallites which was confirmed by uniform distribution of crystallites in the glass ceramic microstructure. It was seen that the dielectric constant increases slowly up to the Curie temperature thereafter with increase in temperature it decreases rapidly. This can be explained as the frequency of applied electric

field becomes equivalent to resonant frequency for ionic polarization process, the simultaneous increase in oscillation amplitude causes an increase of dielectric constant. With further increase in frequency, ionic mechanism stops following the applied field and dielectric constant drops.

1 mol. % addition of  $\text{La}_2\text{O}_3$  in BST glass ceramic causes a reduction in the Curie temperature. This reduction is may be due to smaller ionic radii of La as compared to that of Ba and Sr as reported [3]. Thus  $\text{La}_2\text{O}_3$  is quite important in lowering the “Curie temperature” of ferroelectric “BST” (borosilicate glass ceramics), the dielectric value is also increases due to the addition of  $\text{La}_2\text{O}_3$ . The  $\text{La}_2\text{O}_3$  in BST glass ceramic produces n-type semi conductivity due to donor doping through an electronic compensation mechanism. Glass ceramic morphology sample comprises of semiconducting crystalline phases along with insulating glass matrix. The non-ohmic response to the AC field is attributed to blocking of conduction electrons at the crystal–glass interfaces which causes an interfacial polarization. This interfacial polarization helps in obtaining high dielectric constant values.

Addition of  $\text{La}_2\text{O}_3$  in BST glass ceramics not only showed a marked increase in the dielectric constant but also reduces the dielectric loss, due to the incorporation of trivalent  $\text{La}^{3+}$ -ions ( $1.36 \text{ \AA}$ ) into divalent  $\text{Ba}^{2+}$  ( $1.61 \text{ \AA}$ ) sites effectively stabilize the oxygen ions in the lattice. As the Ba–O bonds is weaker than the La–O bond, the  $\text{La}^{3+}$  inclusions would restrain the movement of oxygen vacancies. The rise in the dielectric constant was due the “interfacial polarization” and the “space charge polarization” which becomes apparent as a result of the conductivity difference between various phases of residual glass and crystalline phases.

**Blocking factor:** This factor gives the fraction of charge that is blocked at grain and grain-boundary interface with respect to total number of charges present. On further rise in temperature, there is an increase in blocking factor. Apparently, Lanthanum oxide can also contribute to the increase in the blocking factor. The rise in the blocking factor leads to the fall in the ionic mobility in the grain and the grain-boundary interface. According to the plot  $Z''$

versus  $\text{Log } f$ , the sharp decrease of  $Z''$  points towards a large contribution of the space charge polarization at interfaces of high resistivity. It shows that the semiconducting nature of the matrix is due to the diffusion of La ions within the matrix. The peak is observed at a high temperature and is shifted towards higher frequency side, which indicates the “relaxation due to polarization”. [4]

J. Wang *et al.* [5] studied the preparation as well as dielectric characterization of BST glass ceramics which were sintered with the help of precursors derived through sol-gel route, and found out that perovskite BST phase was precipitated at  $700^\circ\text{C}$ , and the size of BST grains have reduced and also they found that grain boundaries were not distinct. With the increase in the temperature, the grain growth increased. They also found that sintering temperature in case of BST glass ceramic is much lower as compared to the BST ceramic, due to the presence of glassy phase in the glass ceramic sample the dielectric permittivity was seen to be decreased, but upon increasing the sintering temperature, the considerable increase in the dielectric permittivity and lowering of the dissipation factor observed.

S. Lahiry, and A. Mansingh [6] studied the dielectric properties of barium strontium titanate thin films which were prepared through sol-gel route, via a technique in which the BST films were deposited over a substrate made up of silicon. They observed the films which were deposited using the sol-gel technique was amorphous in nature. The films were crystallized at  $700^\circ\text{C}$  for 1 hour. The dielectric measurements were performed to measure the dielectric constant as well as the dissipation factor with varying frequency and temperature in the range of  $-180^\circ\text{C}$  to  $150^\circ\text{C}$  and 0.1 to 100 kHz. It was seen that small dispersions in dielectric constant occurred for all the compositions. It was also observed that the dispersions were higher at elevated temperature than at room temperature. It was concluded that on increasing the strontium content the transition temperature is considerably decreased and also leads to destabilization of the ferroelectric state.

Ting Wu *et al.* [7] prepared  $\text{Sr}_x\text{Ba}_{1-x}\text{TiO}_3$  ( $x=0.50\text{--}0.70$ ) ceramics and systematic investigation was carried out to check the change in the microstructures, energy storage properties and dielectric relaxation behaviour for the above mentioned composition upon varying Sr/Ba ratio. Scanning electron microscopy observations concluded that increasing mole fraction of Sr inhibited grain size. The highest energy was obtained by  $\text{Sr}_{0.6}\text{Ba}_{0.4}\text{TiO}_3$  ceramics ( $0.3629 \text{ J/cm}^3$ ). This was attributed to the increase of average breakdown strength resulting from the decrease of grain size and the optimization of microstructure. To study the influence of Sr/Ba ratio on the dielectric relaxation behaviour, activation energy was calculated from the relaxation of dielectric loss, and the complex impedance spectra by the Arrhenius relationship, respectively. A decrease of grain size resulting in more grain boundaries, and difficulty of transferring charge and making an orientation under external electric field were indicated. At the same time, more defects existed at grain boundary and accelerated the thermally activated motions of defects, leading to an increase in activation energy.

It is concluded that the Sr/Ba ratio has an enormous influence on microstructures, energy storage properties and dielectric relaxation behaviour of BST ceramics. Firstly, the inhibition of grain size by the increase of Sr/Ba ratio was proved by the SEM micrographs. The highest energy density was showcased by the samples of BST60 ceramics. This property was attributed to the increase of breakdown strength resulting from the optimization of microstructure. Secondly, the activation energy for the relaxation mechanism (calculated from the relaxation of dielectric loss and the complex impedance spectra increased because of the decrease in grain size. This can be explained as follows: due to the higher grain boundary in the BST ceramics (on increasing Sr/Ba ratio), it is difficult to spread charge and make an orientation under external electric field. At the same time, the decrease of grain size leads to more defects at grain boundary, which accelerates the thermally activated motions of defects,

and increases the activation energy. The data obtained from these results about  $\text{Ba}_x\text{Sr}_{1-x}\text{TiO}_3$  ceramics find application in capacitor ceramics.

G.H. Jaffari *et al.* [8] did a comparative study on the frequency response of a bulk barium strontium titanate which were sintered at two different temperatures, one at  $1000^\circ\text{C}$  and the other at  $1400^\circ\text{C}$ . And it was seen that dielectric properties of the two samples were very different but the crystal structure and the electronic structure were found same for both the samples. They also observed that samples which were sintered at higher temperature showed an enhancement in the dielectric constant and the ferroelectric transitions were non-dispersive, then they studied the dielectric response with respect to varying frequency and temperature, but for the other sample which was sintered at lower temperature it was seen that it showed relaxor like features. Further through microstructural studies it was seen that the sample which was fired at lower temperature showed lower density as compared to the other sample which was annealed at a higher temperature. Finally they concluded that the relaxor behaviour cannot be related directly to composition, the sample porosity and homogeneity must also be taken in to account.

A. K. Yadav *et al.* [9] made an attempt to prepare and study the crystallization and dielectric properties of  $\text{Fe}_2\text{O}_3$  doped barium strontium titanate borosilicate glass by the conventional melt quench method. Various characterization techniques were used like impedance spectroscopy, scanning electron microscope, XRD and DTA, followed by crystallization of the glass samples via heat treatment process using the DTA results, they found the activation energy for crystallization  $818 \pm 1.6 \text{ kJ mol}^{-1}$ , they found that on addition of  $\text{Fe}_2\text{O}_3$  the dielectric constant increased up to  $\sim 107070$  for glass ceramic sample which was heat treated for 6 hours, this increase in the dielectric constant value is the result of the space charge polarization which arises due to the difference in conductivity between the insulating grain

boundary and the semiconducting grain.  $\text{Fe}_2\text{O}_3$  played a variety of roles such as it helped to increase the activation energy, reduces the dielectric loss and also acts as a nucleating agent.

S. Hashimoto *et al.* [10] studied the conductivity and expansion properties of  $\text{Sr}_{0.7}\text{La}_{0.3}\text{TiO}_{3-\alpha}$  which was prepared under reducing atmosphere. They estimated the lattice parameter from the Vegard's law between  $\text{SrTiO}_3$  and  $\text{LaTiO}_3$ , but the lattice parameter value was found larger than they expected due to reductive expansion. At  $1000^\circ\text{C}$ ,  $p_{\text{O}_2} = 10^{-13}$  Pa the conductivity of the specimen was  $100 \text{ S cm}^{-1}$ , however after an oxidation-reduction cycle the conductivity was not preserved. They also found that with increasing partial pressure of oxygen the conductivity drastically dropped. The thermal expansion coefficient was found to be around  $11.8 \times 10^{-6} \text{ K}^{-1}$  in 9%  $\text{H}_2/\text{N}_2$ , upon oxidation the chemical expansion reached up to 0.51%, along with partial pressure of oxygen changing from  $10^{-11}$  Pa to  $2 \times 10^4$  Pa (air) at  $1000^\circ\text{C}$ .

P. Blenow *et al.* [11] studied the defect as well as electric transport properties of  $\text{SrTiO}_3$ , they prepared samples using a modified glycine nitrate combustion method. By using XRD, SEM, TGA, and XANES the defect structure and the phase purity of the materials were analysed. They observed that the electrical conductivity of the niobium doped strontium titanate sample decreased with increase in temperature. The sample also showed a phonon scattering mechanism. The results which were found were quite similar to that of the defect chemistry model of donor-doped  $\text{SrTiO}_3$ , in this case when samples are sintered in reducing atmosphere the charge compensation changes from Sr vacancy compensation to the electronic type. Ti is the only species that is reduced to a lower oxidation state (from  $\text{Ti}^{4+}$  to  $\text{Ti}^{3+}$ ) as indicated by XANES AND TGA. Niobium improved the overlap of the Ti atomic orbitals, according to the XANES results, which speaks about the positive effects of Nb on the electronic conductivity of  $\text{SrTiO}_3$  doped with Nb.

J. Karaczewski *et al.* [12] studied the electrical as well as structural properties of  $\text{SrTiO}_3$  doped with  $\text{Nb}_2\text{O}_5$ , they prepared the samples by conventional solid state reaction method.



Thermally activated to metallic behaviour transitions were seen in the samples which were reduced in hydrogen atmosphere at around 1400°C. At 650°C electrical conductivity value seemed to be maximum ( $55 \text{ Scm}^{-1}$ ). They observed that the reducing temperature and the porosity of the sample highly affected the change in the electrical properties of the Nb-doped SrTiO<sub>3</sub> ceramic sample, hence it was concluded that Nb-doped SrTiO<sub>3</sub> can be used as a new SOFC anode material because despite having porosity of around 30% the conductivity level is sufficient.

### **3. EXPERIMENTAL METHODS**

The fabrication of glass ceramic involves the production of a homogenous glass and then conversion of this glass into a microcrystalline glass ceramic by application of controlled heat treatment process.

#### **3.1 MATERIALS**

Reagent grade chemicals such as BaCO<sub>3</sub> (Ranbaxy, 97%), K<sub>2</sub>CO<sub>3</sub> (Merck, 99.9%), H<sub>3</sub>BO<sub>3</sub> (Merck, 99.5%), TiO<sub>2</sub> (Merck,  $\geq 99\%$ ), SiO<sub>2</sub> (TRL Belpahad, 98%), SrCO<sub>3</sub> (S.D. Fine Chemical Ltd., 99%) and Nb<sub>2</sub>O<sub>5</sub> (Merck, 99.9%), were used for the preparation of glass as well as glass ceramic samples.

#### **3.2 GLASS PREPARATION**

Firstly, batch calculation was done for 20 gm of the sample so the calculated amount of raw materials (chemicals) were weighed and mixed using an agate mortar employing a wet mixing technique with acetone as a mixing media, then the powder mixture is transferred in a platinum crucible and melted in an electric raising hearth furnace with melting temperature at 1350°C, The liquid melt is maintained inside the furnace for 2 hours for homogenization and refining, after that the melt is poured out into a mild steel plate while a top plate is immediately pressed over the melt to achieve high rate of cooling. Then the glass sample was subjected to

annealing at a temperature range of 400- 450 °C and were cooled immediately after annealing. The amorphosity of glass ceramic was checked using X-Ray diffraction.

### **3.3 INFRARED SPECTROSCOPY**

A laboratory instrument that uses this infrared spectroscopy technique is known as FTIR (Fourier transform infrared spectrometer). Between the microwave and infrared region of the electromagnetic spectrum lies the infrared region, the molecular as well as the atomic structure within the specimen is studied by the infrared spectroscopy. The broadening of the bands in the Infra-red spectra of the glasses and fluctuations in intensity and merging of the bands is caused due to the disorder in the mutual arrangement of the groups, and this disorder in the groups is caused due to vibration of different groups. In order to study the structure and chemical bonding the glassy materials FTIR analysis is a useful tool. So we used the Perkin Elmer Spectrum version 10.4.00 for doing our FTIR analysis for both of our glass samples. The glass powder was mixed with KBr in 1:10 ratio and then pellets were pressed. FTIR spectra was taken with the varying wavenumber from 400 to 4000  $\text{cm}^{-1}$ .

### **3.4 DIFFERENTIAL SCANNING CALORIMETRY ANALYSIS (DSC)**

DSC studies of our glass samples were done using 100 mg of the powder sample with the help of “NETZSCH DSC/TG Analyser”. The DSC was done from room temperature to 700°C, employing a heating rate of 10°C/min. DSC results provided us with a variety of information such as crystallization temperature for the possible crystalline phases, glass transition temperature. The structural changes or the chemical reactions within the glass is the result of the exothermic and endothermic peaks that is the evolution and absorption of heat.

### **3.5 DENSITY STUDIES**

Density of both the glass as well as glass ceramic samples were recorded using Archimedes principle, which uses the following formula;

Bulk density =  $(D / (W-S)) \times$  density of water

Where, D= dry weight of the sample, W= soaked weight of the sample, S= suspended weight of the sample in water.

### **3.6 GLASS CERAMIC PREPARATION**

Based upon the DTA studies the glass samples were heat treated for crystallization of glasses and transforming them to glass ceramic. By varying the holding time and crystallization temperature the formation of the crystalline phases were controlled. The glasses were heat treated in a muffle furnace from room temperature to the desired temperature incorporating a heating rate of 5°C/minute, the samples were kept on a pure alumina crucible which was then inserted in to the furnace. The temperature of crystallization is marked by the DTA peak and when the samples reaches the desired crystallization temperature it is maintained at that temperature for 3 hours. After the crystallization process is over, the samples are furnace cooled to room temperature.

### **3.7 IDENTIFICATION OF CRYSTALLINE PHASES**

After the crystallization of the glass samples the glass ceramic samples were grinded to fine powder in order to perform the X-Ray diffraction analysis, using a “Rigaku Ultima 4” X-Ray diffractometer employing Cu K $\alpha$  radiation ( $\lambda = 0.15406$  nm) within  $2\Theta$  value of 10 to 90°. The observed XRD patterns were indexed using standard JCPDS files found in the HighScorePlus database. The crystallization behaviour of various glass samples was understood by the systematic study of crystalline phases present in the glass ceramic samples with respect to their heat treatment schedules.

### **3.8 MICROSTRUCTURAL STUDIES**

The glass ceramic samples were polished using sand papers with grid 240 and grid 220 to get a smooth surface, and then with the help of diamond paste (3 $\mu$ m) and lap cloth, final polishing was achieved to give the glass surface a mirror like finish. Then these polished glass samples were used for SEM analysis. Samples for SEM analysis were prepared by sputtering

Au film on to the polished glass ceramic surface to prevent charge build-up at the surface. SEM micrographs of the samples were recorded at different magnifications using Field Emission Scanning Electron Microscope (NOVA NanoSEM/FEI) operating at 30kV.

### **3.9 DIELECTRIC MEASUREMENT**

The glass ceramic samples were first made in to a desired rectangular shape with thickness of about 1mm followed by polishing with the help of grid 240 and grid 220 sand papers for attaining smooth surfaces, Electroding of the samples were done using conductive paint, Ag paste was applied on the glass ceramic samples and then it is dried at around 100°C for 1 hour followed by curing at 600°C for 1 hour using a custom made platinum sample holder enclosed in an alumina tube, which is shielded from outside disturbance using a metallic jacket. The whole system was connected to “HIOKI 3532-50 LCR HITESTER”, dielectric parameters like capacitance (C), dielectric constant ( $\epsilon_r$ ), and dielectric loss (D), were measured with respect to varying frequency and temperature. Measurements were recorded in the temperature range of 30-250°C and with a frequency range of 100Hz-1MHz at a temperature interval of 10°C. After the measurement is over the dielectric constant of the sample were recorded using the relation;

$$\epsilon_r = C.t / (\epsilon_0.A)$$

Where C is the capacitance,  $\epsilon_0$  is the permittivity of the free space ( $\epsilon_0 = 8.854 \times 10^{-12}$  F/m)

t is the thickness of the glass ceramic sample in meter

A is the area of the glass sample in square meter

And the dielectric loss ( $\tan\delta$  or D) values were directly determined by the Impedance Analyser.

## **4. RESULTS AND DISCUSSION**

### **4.1 XRD ANALYSIS**

#### **BEFORE CRYSTALLIZATION**

After the preparation of three different glass samples by the conventional melt quench method first one having the composition  $[(\text{Ba}_{0.2}\text{Sr}_{0.8})\cdot\text{O}\cdot\text{TiO}_2]-[2\text{SiO}_2-\text{B}_2\text{O}_3]-[\text{K}_2\text{O}]$  which was quenched on a preheated graphite plate, second one having the same composition  $[(\text{Ba}_{0.2}\text{Sr}_{0.8})\cdot\text{O}\cdot\text{TiO}_2]-[2\text{SiO}_2-\text{B}_2\text{O}_3]-[\text{K}_2\text{O}]$  but quenched at room temperature and the third sample being  $[(\text{Ba}_{0.2}\text{Sr}_{0.8})\cdot\text{O}\cdot\text{TiO}_2]-[2\text{SiO}_2-\text{B}_2\text{O}_3]-[\text{K}_2\text{O}]-0.1 \text{ mol. \%}[\text{La}_2\text{O}_3]$  also quenched at room temperature, their XRD was analysed and it was observed that for the first sample, a broad X-ray hump is observed around  $25-30^\circ$  ( $2\theta$  value) due to the formation of borosilicate glass and thus as glass is amorphous hence it was confirmed that glassy matrix is formed. However, during quenching of the liquid melt on a preheated graphite plate a  $\text{SiO}_2$  (011) peak is observed at  $26.60^\circ$  ( $2\theta$  value) either due to partial crystallization of  $\text{SiO}_2$  or the unreacted  $\text{SiO}_2$  precipitate from the liquid melt, which can be very well observed from the **Fig. 2**. For the second glass sample having the same composition but quenched at room temperature it was observed that broad X-ray hump is observed around  $25-34^\circ$  ( $2\theta$  value) due to formation of borosilicate glassy phase, which can be very well observed from the **Fig. 3**. For the third glass sample it was observed that a broad X-ray hump is observed around  $25-34^\circ$  ( $2\theta$  value) due to formation of borosilicate glass. It appears from the XRD that the desired  $\text{Sr}_{0.8}\text{Ba}_{0.2}\text{TiO}_3$  phase remains in the amorphous form within the borosilicate glassy matrix, which can be very well observed from the **Fig. 4**.

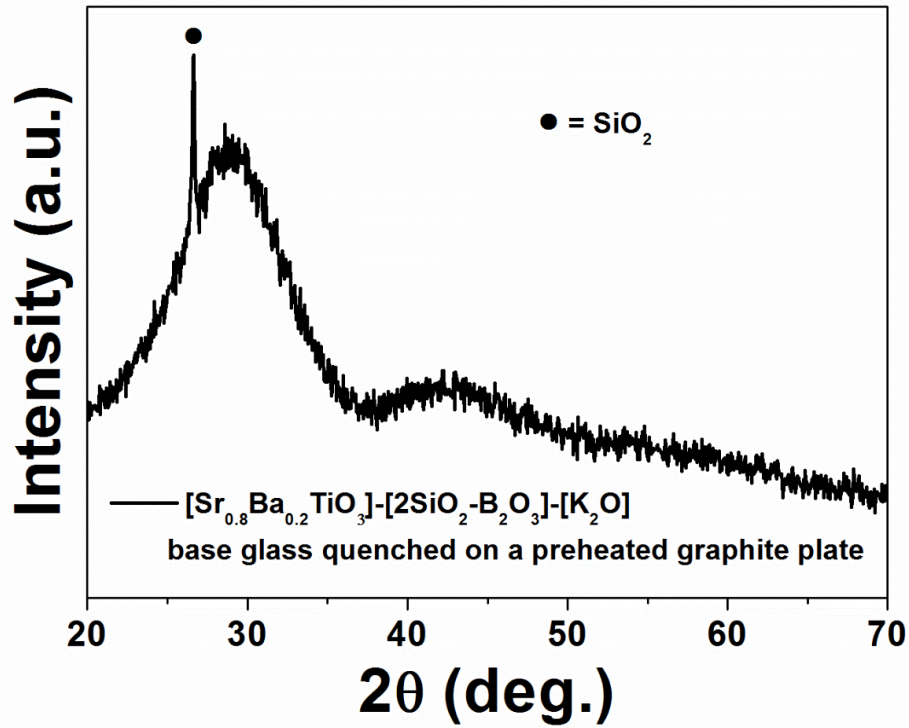


**Fig. 2** XRD pattern of  $[(\text{Ba}_{0.2}, \text{Sr}_{0.8})\text{O}\cdot\text{TiO}_2]\text{-}[2\text{SiO}_2\text{-B}_2\text{O}_3]\text{-}[\text{K}_2\text{O}]$  glass quenched on a preheated graphite plate

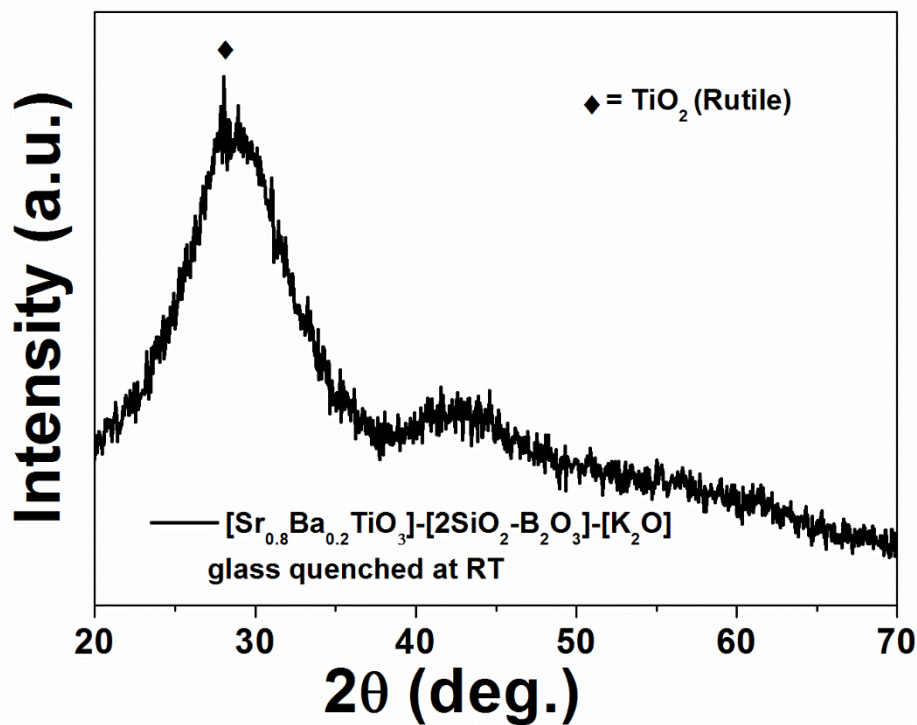


**Fig. 3** XRD pattern of  $[(\text{Ba}_{0.2}, \text{Sr}_{0.8})\text{O}\cdot\text{TiO}_2]\text{-}[2\text{SiO}_2\text{-B}_2\text{O}_3]\text{-}[\text{K}_2\text{O}]$  glass quenched at room temperature

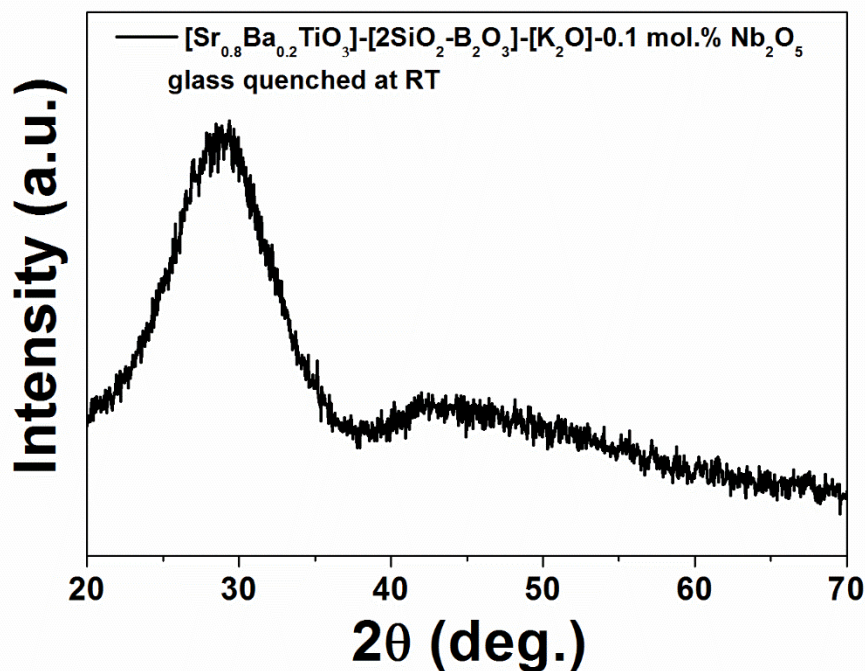


**Fig. 4** XRD pattern of  $[(\text{Ba}_{0.2}\text{Sr}_{0.8})\cdot\text{O}\cdot\text{TiO}_2]\text{-}[2\text{SiO}_2\text{-B}_2\text{O}_3]\text{-}[\text{K}_2\text{O}]\text{-}0.1\text{ mol \% } [\text{Nb}_2\text{O}_5]$  glass quenched at room temperature

#### 4.2 INFRARED SPECTROSCOPY ANALYSIS

**Base glass:** From **Fig. 5** we can see the list of transmittance peaks with respect to their wavenumbers observed in case of the base glass sample having the composition  $\text{Ba}_{0.2}\text{Sr}_{0.8}\text{TiO}_3\text{-}2\text{SiO}_2\text{-B}_2\text{O}_3\text{-K}_2\text{O}$ , quenched at room temperature after the FTIR (Fourier Transform Infrared Spectroscopy) analysis being done in the range  $400\text{-}4000\text{ cm}^{-1}$ . The peaks were observed at 3903, 3853, 3750, 3743, 3648, 3627, 3587, 3567, 3446, 2925, 2528, 968, 414, 404 wavenumbers, respectively. The peak at (1) at  $3750\text{ cm}^{-1}$  is attributed due to water or hydroxyl group. The peak in the range (2), (3), (4) and (5) in the range  $3440\text{-}3470\text{ cm}^{-1}$  corresponds to the stretching of the O-H bond inside the glassy network, this O-H groups are formed at the non-bridging oxygen sites. The presence of the O-H may have be due to the KBr pellet technique. The peak (6) at  $2925\text{ cm}^{-1}$  occurs due to hydrogen bonding in the glassy matrix. The peak (7) at  $968\text{ cm}^{-1}$  indicates the bending of the diborate linkages (B-O-B) in the borate glassy network, and the peaks around  $400\text{ cm}^{-1}$  are result of the vibration of the metal cation. [13]

**Doped glass:** From **Fig. 6** we can see the list of transmittance peaks with respect to their wavenumbers observed in case of the doped glass sample having the composition  $\text{Ba}_{0.2}\text{Sr}_{0.8}\text{TiO}_3\text{-}2\text{SiO}_2\text{-B}_2\text{O}_3\text{-K}_2\text{O-}0.1\text{mol.}\% \text{Nb}_2\text{O}_5$  and quenched at room temperature. After the FTIR (Fourier Transform Infrared Spectroscopy) analysis being done in the range  $400\text{-}4000 \text{ cm}^{-1}$ , peaks were found at  $3858, 3468, 3435, 1642, 1550, 1414, 1000, 712, 588, 552, 457, 442, 427, 417, 410, 405, 402, \text{ cm}^{-1}$  respectively. The transmittance peak **(1)** at  $3435 \text{ cm}^{-1}$  is sharp as its strontium rich samples and these peaks corresponds to the stretching of the O-H bond inside the glassy network, this O-H groups are formed at the non-bridging oxygen sites. The presence of the O-H may be due to the KBr pellet technique. The peaks **(2)**, **(3)**, and **(4)** in the range  $1200\text{-}1650 \text{ cm}^{-1}$  are due to the vibrational mode of the borate network, the vibrational modes of the borate network are mainly due to the asymmetric stretching relaxation of the B-O bond of trigonal  $\text{BO}_3$  units. The peak **(5)** at  $1000 \text{ cm}^{-1}$  is due to the stretching vibration of the B-O-Si linkages. The peak **(6)** at  $712 \text{ cm}^{-1}$  is due to the bending of diborate linkages (B-O-B) in the borate glassy network. In this linkage both the boron atom are tetrahedrally coordinated with triborate super structural units. And the peak **(7)** in the range  $402\text{-}588 \text{ cm}^{-1}$  is mainly due to the vibration of the metal cation ( $\text{Ba}^{2+}, \text{Sr}^{2+}$ ). As we can see there is no peak at  $806 \text{ cm}^{-1}$  it confirms the absence of boroxil ring in the glassy network. [14]

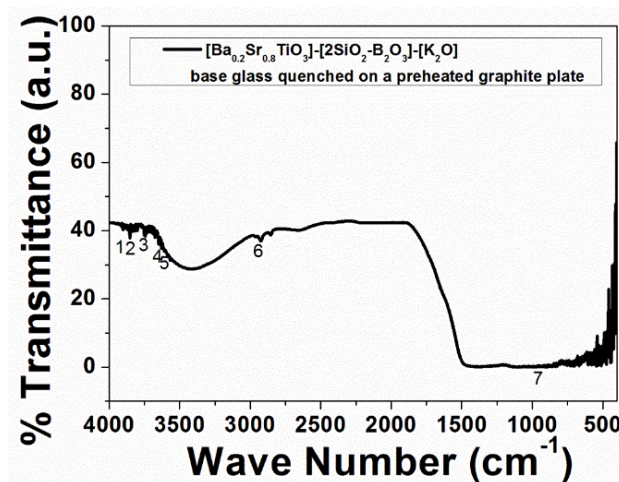


**Fig. 5** FTIR spectra of SBT base glass



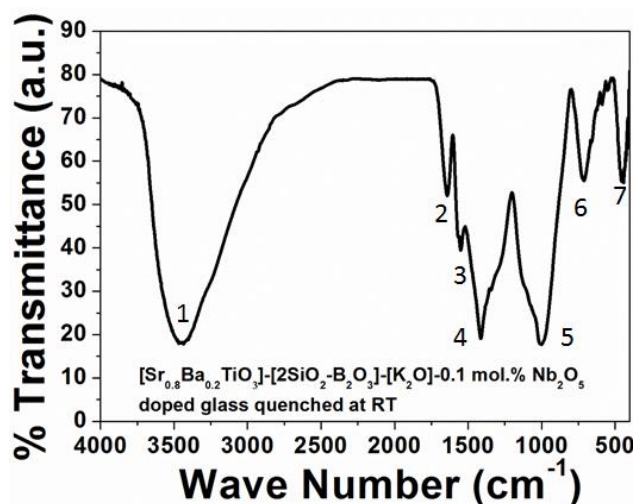


**Fig. 6** FTIR spectra of 0.1 mol % Nb<sub>2</sub>O<sub>5</sub> doped SBT glass

#### 4.3 DIFFERENTIAL SCANNING CALORIMETRY ANALYSIS

Three different glass samples were made using the conventional melt quench method, first one being the base glass that was quenched on a graphite plate at high temperature, having the composition [Ba<sub>0.2</sub>Sr<sub>0.8</sub>TiO<sub>3</sub>-2SiO<sub>2</sub>-B<sub>2</sub>O<sub>3</sub>-K<sub>2</sub>O]. Second one being the base glass quenched at room temperature using mild steel plates having the composition [Ba<sub>0.2</sub>Sr<sub>0.8</sub>TiO<sub>3</sub>-2SiO<sub>2</sub>-B<sub>2</sub>O<sub>3</sub>-K<sub>2</sub>O]. And the third one being the doped glass having the composition [Ba<sub>0.2</sub>Sr<sub>0.8</sub>TiO<sub>3</sub>-2SiO<sub>2</sub>-B<sub>2</sub>O<sub>3</sub>-K<sub>2</sub>O-0.1 mol. % Nb<sub>2</sub>O<sub>5</sub>] quenched at room temperature using mild steel plates. The DSc curve illustrated in the **Fig. 7** it was seen that the ( $T_g$ ) glass transition temperature is at 335°C, and the onset of crystallization temperature was found to be around 564°C, so a temperature is chosen between 745 to 793°C for the crystallization of strontium barium titanate phase in the glassy matrix, temperature is chosen in this range because below 745°C no crystallization will take place and above 793°C the entire sample will be crystallized, so partial crystallization will take place in this temperature range. By partial crystallization we can achieve a structure like expected BST crystals will be embedded in the glassy matrix, which is desirable for a variety of application. As the crystallization temperature is known so maintaining the sample at that very temperature for a prolonged period of time will help to increase the crystal size.

The DSC curve of the second glass sample is illustrated in **Fig. 8** that is base glass which was quenched at room temperature using mild steel plates, it was seen that the ( $T_g$ ) glass transition temperature is at 302°C, and the onset of crystallization temperature was found to be around 564°C, so a temperature is chosen in between 745 to 793°C for the crystallization of strontium barium titanate phase in the glassy matrix, temperature is chosen in this range because below 745°C no crystallization will take place and above 793°C the entire sample will be crystallized, so partial crystallization will occur. By partial crystallization a dual phase of glass ceramics embedded in the glassy matrix can be achieved, which is desirable for a variety of application.

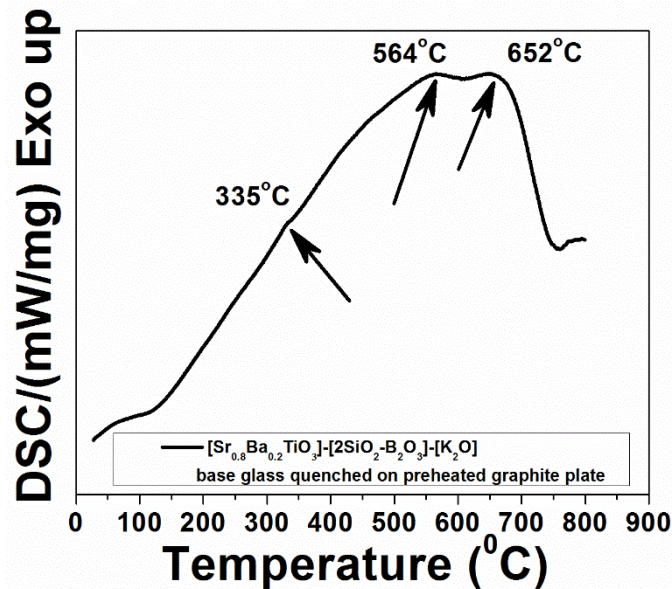


**Fig. 7** DSC scan from room temperature to 800 °C of base glass quenched on preheated graphite plate

The DSC graph for the third glass sample is shown in **Fig. 9** that is doped glass which was quenched at room temp using mild steel plates, it was seen that the ( $T_g$ ) glass transition temperature is at 346°C, and the onset of crystallization temperature was found to be around 555°C, so a temperature is chosen in between 714 to 769°C for the crystallization of strontium barium titanate phase in the glassy matrix, temperature is chosen in this range because below 714°C no crystallization will take place and above 769°C the entire sample will be crystallized,

so as we require partial crystallization hence temperature was chosen in this range. By partial crystallization we can achieve a structure like BST crystals embedded in the glassy matrix, which is desirable for a variety of application.

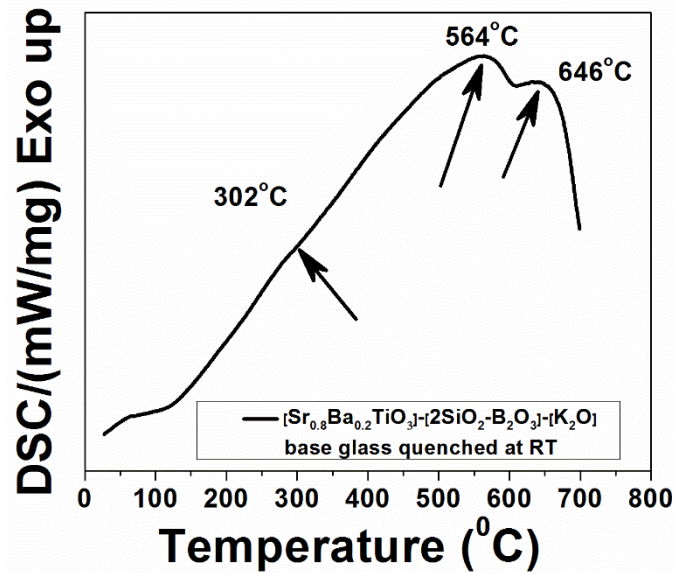


**Fig. 8** DSC study of from room temperature to 700 °C of air quenched base glass sample

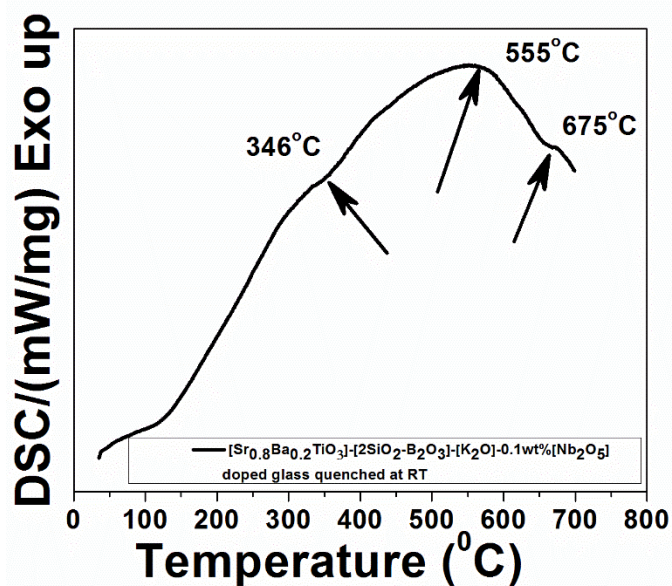


**Fig. 9** DSC study from room temperature to 700 °C of 0.1 mol % Nb<sub>2</sub>O<sub>5</sub> doped glass sample

#### 4.4 DENSITY ANALYSIS

Density studies were carried on for all the three glass samples, first one being the base glass quenched at room temperature having the composition [Ba<sub>0.2</sub>Sr<sub>0.8</sub>TiO<sub>3</sub>-2SiO<sub>2</sub>-B<sub>2</sub>O<sub>3</sub>-K<sub>2</sub>O].

Second one being the base glass quenched at room temperature using mild steel plates having the composition  $[Ba_{0.2}Sr_{0.8}TiO_3-2SiO_2-B_2O_3-K_2O]$ , and the third one being the doped glass having the composition  $[Ba_{0.2}Sr_{0.8}TiO_3-2SiO_2-B_2O_3-K_2O-0.1 \text{ mol. \% } Nb_2O_5]$  quenched at room temperature using mild steel plates, and also taken for the corresponding glass ceramic samples which were prepared after heat treatment at a particular temperature which was determined by the DSC studies. It was seen that the density of the three glass samples lie in the range 2.95-3.21 g/cc, which is listed below in **Table 1**, and the density for the glass ceramic samples were found in the range 2.97-3.29 g/cc. , which is listed below in **Table 2**, it was observed that there is a slight increase in density of the glass ceramic samples, it is expected that this increase is mainly due to the BST crystals precipitated inside the glassy matrix, as we know that glass is amorphous and the structure is disordered where in case crystalline glass-ceramic structure is

**Table 1** Density measurement of the glass samples

GLASS SAMPLES	DRY WEIGHT (D)	SUSPENDED WEIGHT (S)	SOAKED WEIGHT (W)	BULK DENSITY = D/(W-S)	AVERAGE
Doped glass (quenched at room temperature)	1. 0.5243	1. 0.3558	1. 0.5282	1. 3.06	3.057±0.004 g/cc
	2. 0.5263	2. 0.3578	2. 0.5302	2. 3.052	
	3. 0.5278	3. 0.3593	3. 0.5317	3. 3.061	
Base glass (quenched at high temperature)	1. 1.0634	1. 0.7092	1. 1.0643	1. 2.994	2.974±0.02 g/cc
	2. 0.8240	2. 0.5476	2. 0.8271	2. 2.948	
	3. 0.4399	3. 0.2928	3. 0.4404	3. 2.980	
Base glass (quenched at room temperature)	1. 0.6786	1. 0.4709	1. 0.6797	1. 3.25	3.29±0.06 g/cc
	2. 0.1360	2. 0.0958	2. 0.1365	2. 3.341	

ordered, hence causes an increase in the density of the glass ceramic. The glass ceramic density can also be said as an additive function of densities of the glassy phases and various crystalline phases present, which depends on the density of crystalline phase, residual glass and percentage

crystallinity. There are four factors which affect density such as inclusion, temperature at the time of measurement, thermal history, and composition.

**Table 2** Density measurement of the glass ceramic samples

GLASS SAMPLES	DRY WEIGHT (D)	SUSPENDED WEIGHT (S)	SOAKED WEIGHT (W)	BULK DENSITY = D/(W-S)	AVERAGE
Doped glass (quenched at room temperature)	1. 0.4335	1. 0.2899	1. 0.4333	1. 3.023	3.022±0.03 g/cc
	2. 0.1348	2. 0.0895	2. 0.1343	2. 3.088	
	3. 0.4368	3. 0.2924	3. 0.4362	3. 3.037	
Base glass (quenched at high temperature)	1. 0.9878	1. 0.6547	1. 0.9891	1. 2.953	2.95±0.004 g/cc
	2. 1.7033	2. 1.1285	2. 1.7067	2. 2.952	
	3. 1.0070	3. 0.6670	3. 1.0077	3. 2.961	
Base glass (quenched at room temperature)	1. 0.2230	1. 0.1529	1. 0.2222	1. 3.2178	3.210±0.01 g/cc
	2. 0.6702	2. 0.4617	2. 0.6700	2. 3.2174	
	3. 0.2803	3. 0.1923	3. 0.2800	3. 3.1961	

#### 4.4 XRD ANALYSIS

##### AFTER CRYSTALLIZATION

After the formation of glass ceramic all the three samples were analysed first one having the composition  $[(Ba_{0.2}Sr_{0.8}).O.TiO_2]-[2SiO_2-B_2O_3]-[K_2O]$  which was quenched on a preheated graphite plate, second one having the same composition  $[(Ba_{0.2}Sr_{0.8}).O.TiO_2]-[2SiO_2-B_2O_3]-[K_2O]$  but quenched at room temperature and the third sample being  $[(Ba_{0.2}Sr_{0.8}).O.TiO_2]-[2SiO_2-B_2O_3]-[K_2O]-0.1 \text{ mol.}\% [Nb_2O_5]$  also quenched at room temperature, using XRD. It was seen that for the first sample which was crystallized at  $750^\circ\text{C}$ , semi-crystalline phase was formed. However, upon crystallization at  $780^\circ\text{C}$  fully crystalline phase formed. It was also observed that the major phase being  $Sr_{0.744}Ba_{0.2056}TiO_3$  and  $TiO_2$  (Rutile),  $SiO_2$  were present as minor phase as illustrated in **Fig. 10**. The Lattice parameter(s) were calculated by least-square technique. Calculated Lattice parameter(s) of the sample [ $a = 0.39049 \text{ nm}$  and unit cell volume

=  $59.51 \times 10^{-3} \text{ nm}^3$ ] matched quite well with the standard lattice cell parameter(s) [ $a = 0.39250 \text{ nm}$  and unit cell volume =  $60.47 \times 10^{-3} \text{ nm}^3$ ] of  $\text{SrBaTiO}_3$  phase. For the second glass ceramic sample having the same composition but quenched at room temperature it was observed that the required SBT phase is not precipitated inside the glassy matrix instead we get  $\text{Sr}_2\text{TiSi}_2\text{O}_8$ ,  $\text{SiO}_2$ , and  $\text{KBSi}_2\text{O}_6$  phase shown in **Fig. 11**. However it is expected that as the required phase has not formed because it might require much higher crystallization temperature. The energy barrier in this case might have been higher for the formation of SBT phase in comparison to the pre heated graphite plate quenched glass ceramics. For the third sample it was observed that the major phase is  $\text{Sr}_{0.744}\text{Ba}_{0.256}\text{TiO}_3$ , and  $\text{SiO}_2$ ,  $\text{Ba}_6\text{Nb}_2\text{O}_{11}$  as minor phase, depicted in **Fig. 12**. Lattice parameter(s) were calculated by least-square technique. Calculated Lattice parameter(s) of the sample [ $a = 0.393229 \text{ nm}$  and unit cell volume =  $60.80 \times 10^{-3} \text{ nm}^3$ ] matched quite well with the standard lattice cell parameter(s) [ $a = 0.39250 \text{ nm}$  and unit cell volume =  $60.47 \times 10^{-3} \text{ nm}^3$ ] of  $\text{SrBaTiO}_3$  phase. Hence from the above XRD analysis it can be deduced that we obtained the desired  $\text{SrBaTiO}_3$  phase at  $750^\circ\text{C}$ , so it is expected that due to doping of  $\text{Nb}_2\text{O}_5$ , the crystallization temperature decreased and the desired phase thus obtained at a much lower temperature compared to the un-doped samples, where  $\text{Nb}_2\text{O}_5$  acts as crystallizing agent.

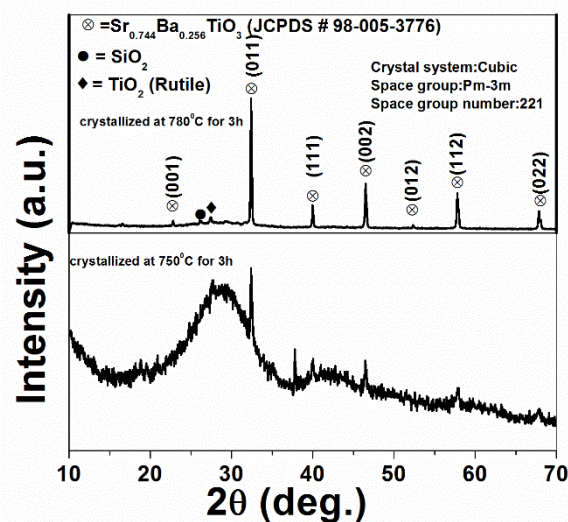


**Fig. 10** XRD pattern of  $[(\text{Ba}_{0.2}\text{Sr}_{0.8})\text{O} \cdot \text{TiO}_2] - [2\text{SiO}_2 - \text{B}_2\text{O}_3] - [\text{K}_2\text{O}]$  glass sample quenched on a preheated graphite plate and then crystallized at  $750^\circ\text{C}$  as well as at  $780^\circ\text{C}$  for 3h in air

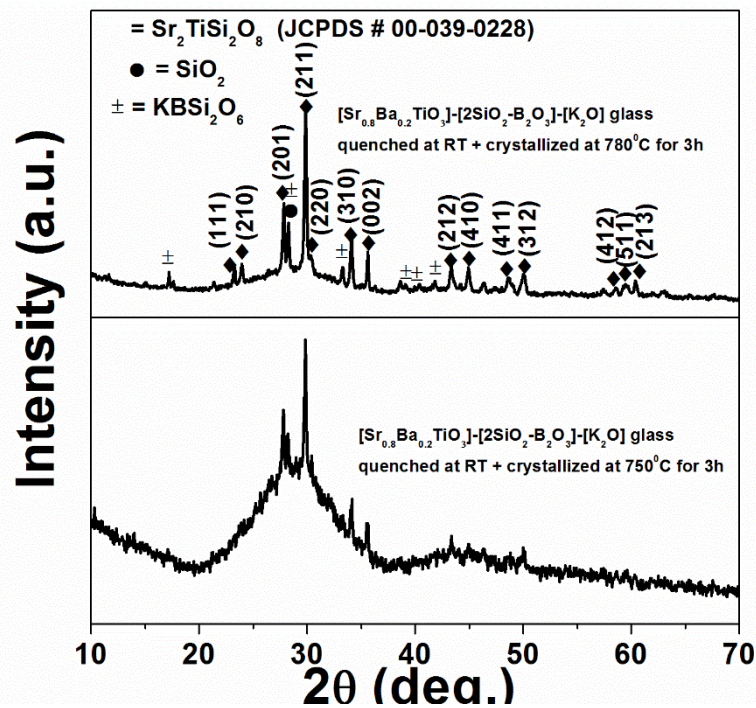


**Fig. 11** XRD pattern of  $[(\text{Ba}_{0.2}\text{Sr}_{0.8})\text{O.TiO}_2]\text{-}[\text{2SiO}_2\text{-B}_2\text{O}_3]\text{-}[\text{K}_2\text{O}]$  glass sample quenched at room temperature and then crystallized at 750°C as well as at 780°C for 3h in air

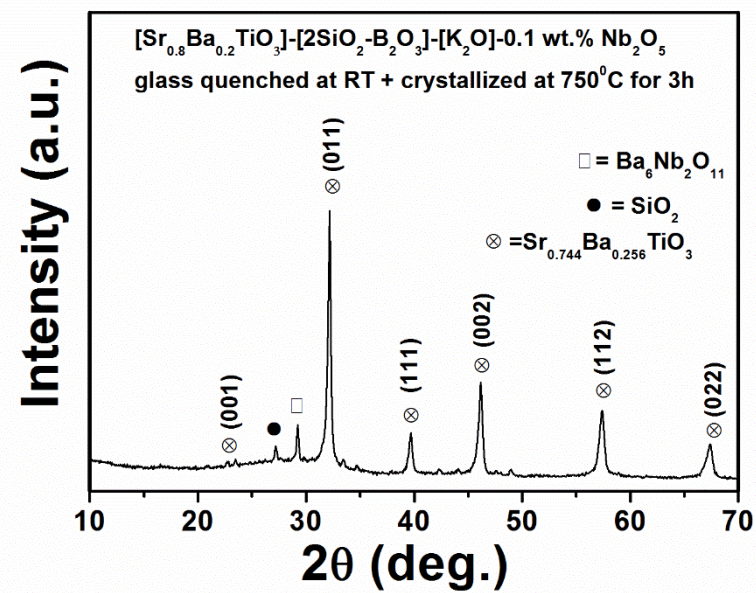


**Fig. 12** XRD pattern of  $[(\text{Ba}_{0.2}\text{Sr}_{0.8})\text{O.TiO}_2]\text{-}[\text{2SiO}_2\text{-B}_2\text{O}_3]\text{-}[\text{K}_2\text{O}]\text{-}0.1 \text{ mol}\% \text{ [Nb}_2\text{O}_5]$  glass sample quenched at room temperature and then crystallized at 750°C for 3h in air

#### 4.6 SCANNING ELECTRON MICROSCOPE ANALYSIS (SEM)

Through this SEM analysis the surface morphology of both the glass ceramic samples were recorded, first being the SBT base glass having the composition  $[(\text{Ba}_{0.2}\text{Sr}_{0.8})\text{O.TiO}_2]\text{-}$

[2SiO<sub>2</sub>-B<sub>2</sub>O<sub>3</sub>]-[K<sub>2</sub>O] and second one being the 0.1 mol. % Nb<sub>2</sub>O<sub>5</sub> doped SBT glass ceramics having the composition [(Ba<sub>0.2</sub>Sr<sub>0.8</sub>)O.TiO<sub>2</sub>]-[2SiO<sub>2</sub>-B<sub>2</sub>O<sub>3</sub>]-[K<sub>2</sub>O]-0.1 mol. % [Nb<sub>2</sub>O<sub>5</sub>]. The detailed microstructural analysis of both samples were showed by SEM. And the distribution of the all the elements present in the microstructure were obtained by the Elemental X-Ray mapping results. Electron Dispersive Spectroscopy (EDS) results obtained shows the quantitative analysis of the microstructures present in the samples. **Fig. 13** illustrate the surface morphology of SBT base glass ceramic, and it was observed that dendritic morphology is observed as well as flower-like, and needle shaped crystals are observed in the microstructure. The detailed composition of the dendritic, flower-like, and needle shaped crystals are determined by the elemental X-ray mapping which is shown in **Fig. 18**. It was observed that the flower-like crystals are rich in strontium as EDS analysis shows that in flower-like crystals Sr<sup>2+</sup>/Ti<sup>4+</sup> ratio is ~0.7 which matches with the ratio of Sr<sup>2+</sup>/Ti<sup>4+</sup> (0.75) in the Sr<sub>0.744</sub>Ba<sub>0.256</sub>TiO<sub>3</sub> composition which can clearly be seen in the **Fig. 14**. So, it can be concluded that major phase formed in the flower like crystal structure was Sr<sub>0.744</sub>Ba<sub>0.256</sub>TiO<sub>3</sub>. In the case of needle-like crystal a mixed composition of Sr, Ti, K, B, O was observed. The result was similar according to EDS analysis which is shown in **Fig. 15**. **Fig. 16** shows the EDS analysis of the matrix and confirmed that borosilicate matrix is preserved. EDS analysis of dendritic morphology illustrated in **Fig. 17** showed that SrTiO<sub>3</sub> phase was formed. From the **Fig. 19**, we can see the surface morphology of 0.1 mol. % Nb<sub>2</sub>O<sub>5</sub> doped SBT glass ceramics having the composition [(Ba<sub>0.2</sub>Sr<sub>0.8</sub>)O.TiO<sub>2</sub>]-[2SiO<sub>2</sub>-B<sub>2</sub>O<sub>3</sub>]-[K<sub>2</sub>O]-0.1[La<sub>2</sub>O<sub>3</sub>]. It is evident that irregular shaped crystals were formed in the microstructure after controlled crystallization. The irregular shaped crystals are mixed phase of SrBaTiO<sub>3</sub> and Ba<sub>6</sub>Nb<sub>2</sub>O<sub>11</sub>. According to the Elemental X-ray mapping shown in the **Fig. 22** it was revealed that irregular shaped crystals (islands) are Sr, Ba, Nb, and Ti rich composition. Boron and Silicon are rich in the matrix. EDS analysis of both irregular shaped crystals and the matrix phase shown in **Fig. 20 and 21**, respectively, confirmed



that irregular shaped crystals are mixed phase of  $\text{SrBaTiO}_3$  and  $\text{Ba}_6\text{Nb}_2\text{O}_{11}$  whereas the matrix phase has got mixed composition.

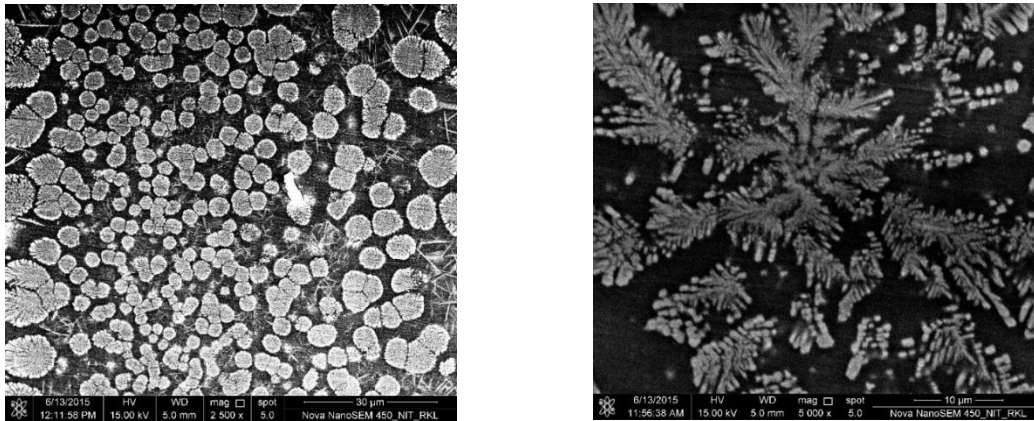


**Fig. 13** SEM images of SBT base glass ceramic

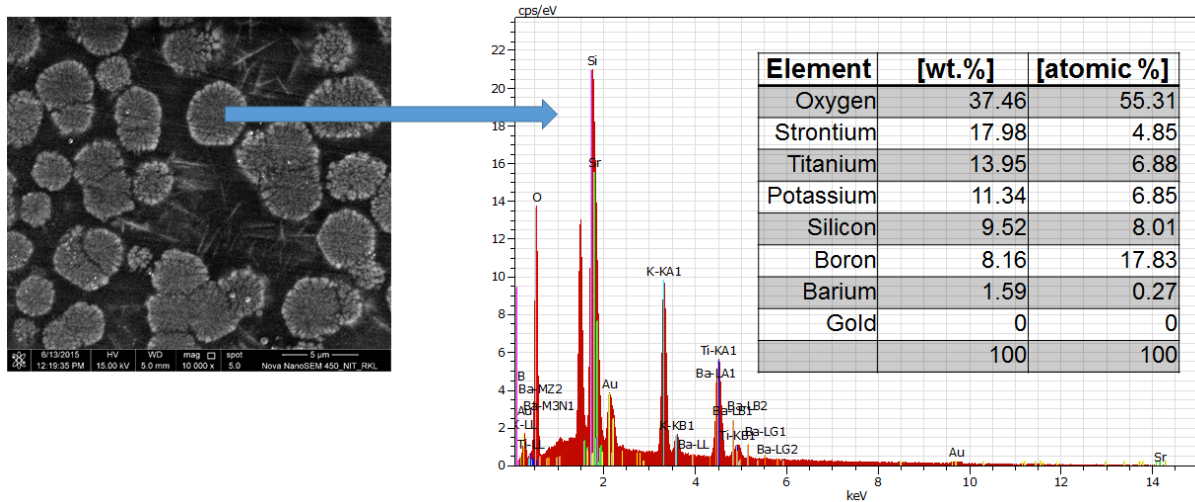


**Fig. 14** EDS analysis of flower like crystal found in the microstructure

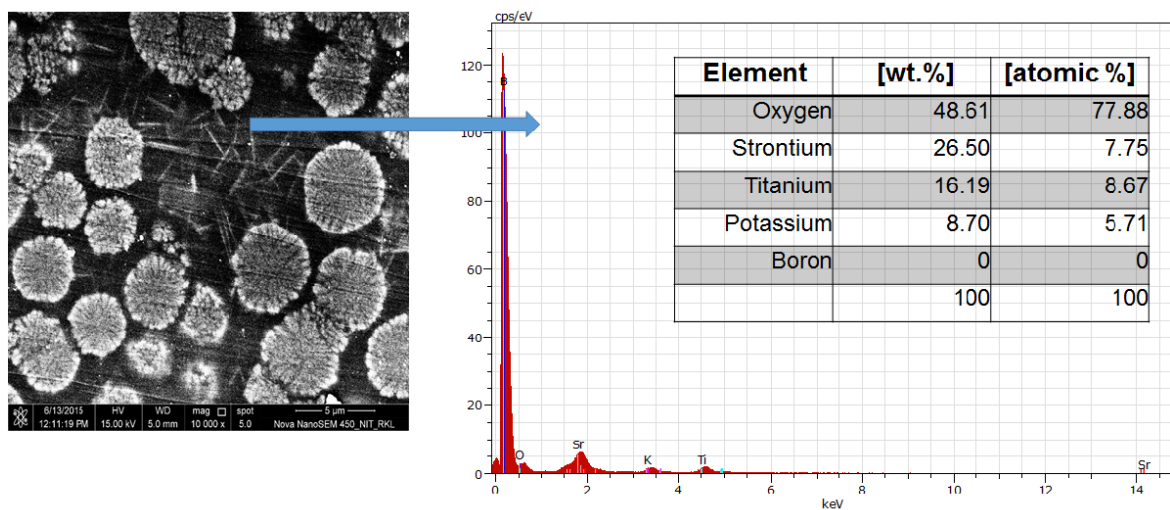


**Fig. 15** EDS analysis of needle like crystal found in the base glass ceramic

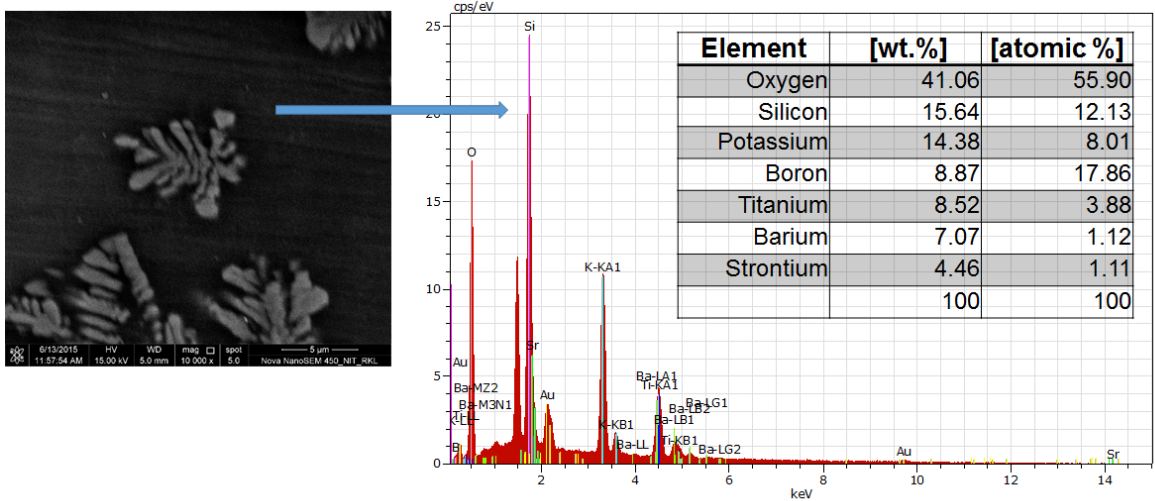


**Fig. 16** EDS analysis of the matrix phase of base glass ceramic

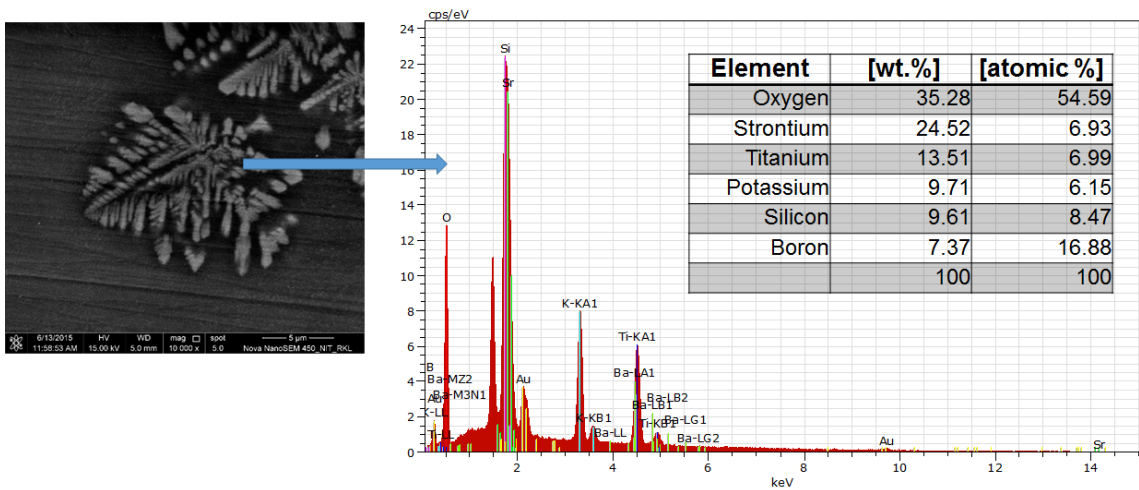


**Fig. 17** EDS analysis of dendritic microstructure

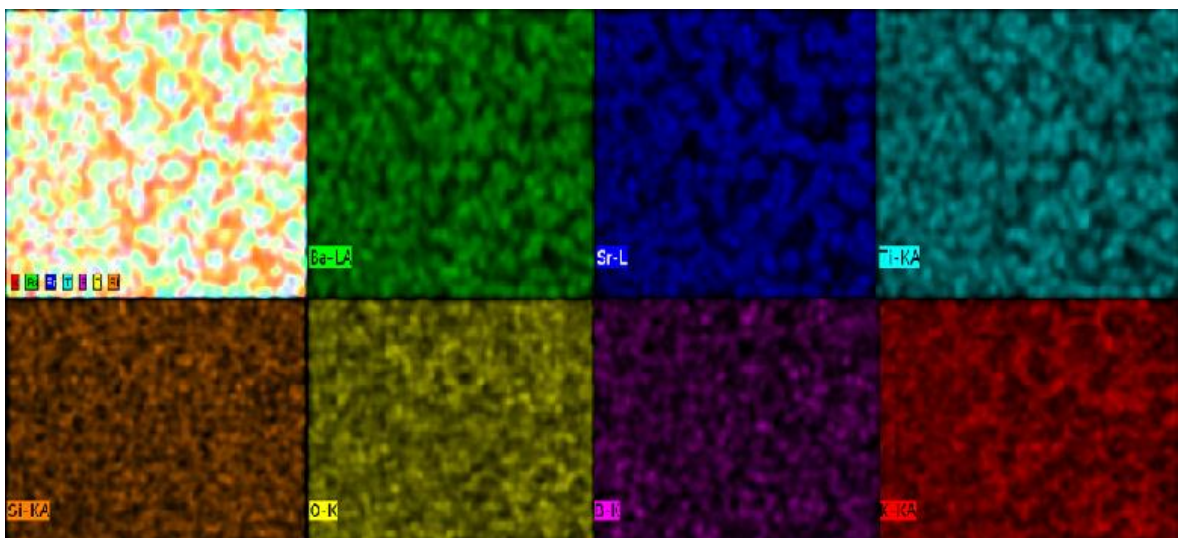


**Fig. 18** Elemental X-ray mapping showing the distribution of elements from SBT base glass ceramic

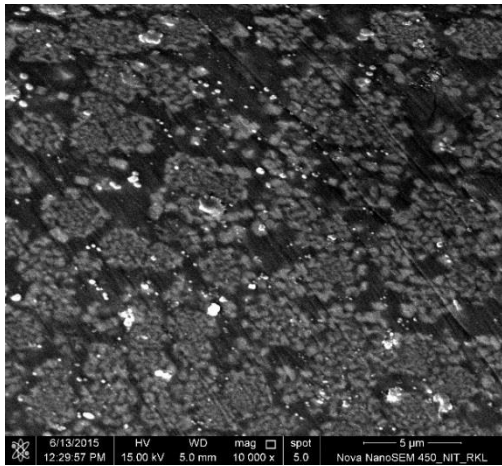


**Fig. 19** SEM image of 0.1mol % Nb<sub>2</sub>O<sub>5</sub> doped glass ceramic

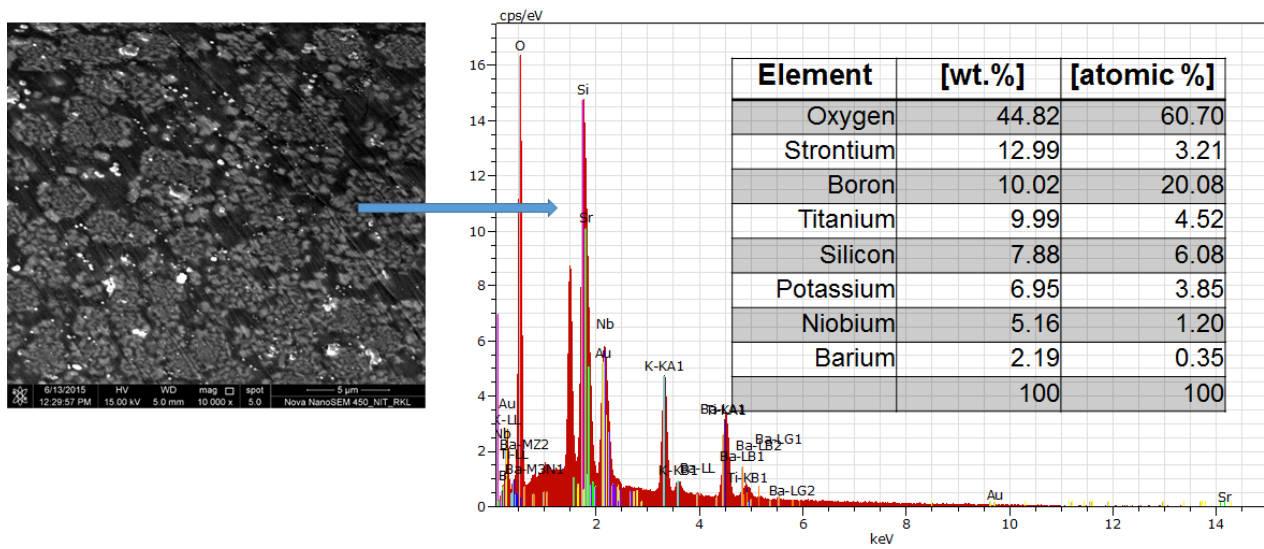


**Fig. 20** EDS analysis for irregular shaped crystals in the microstructure

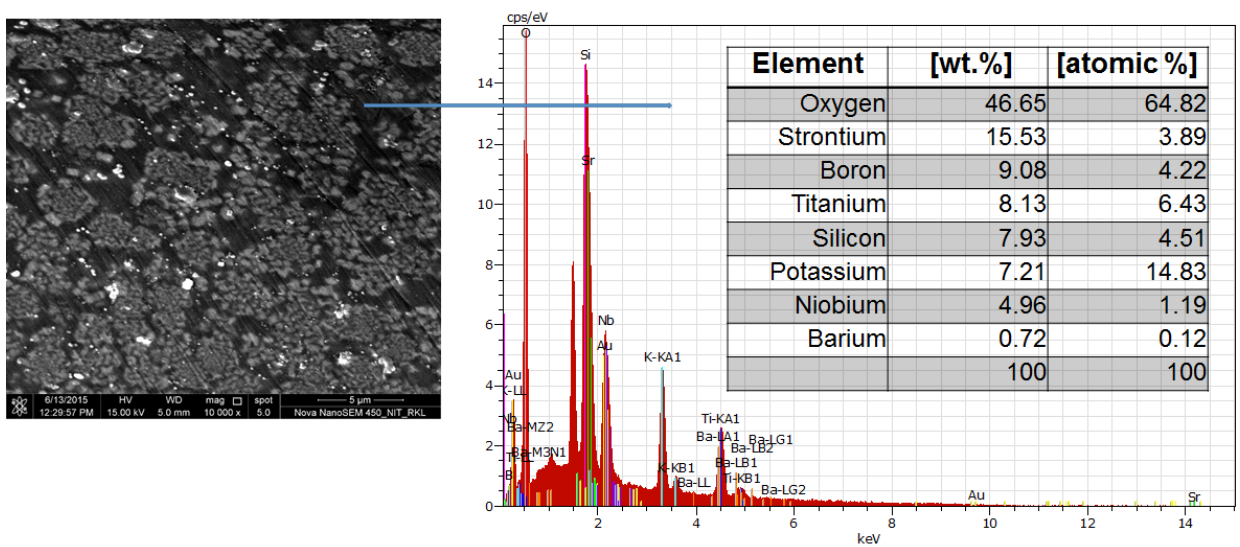


**Fig. 21** EDS analysis of the matrix phase for doped glass ceramic

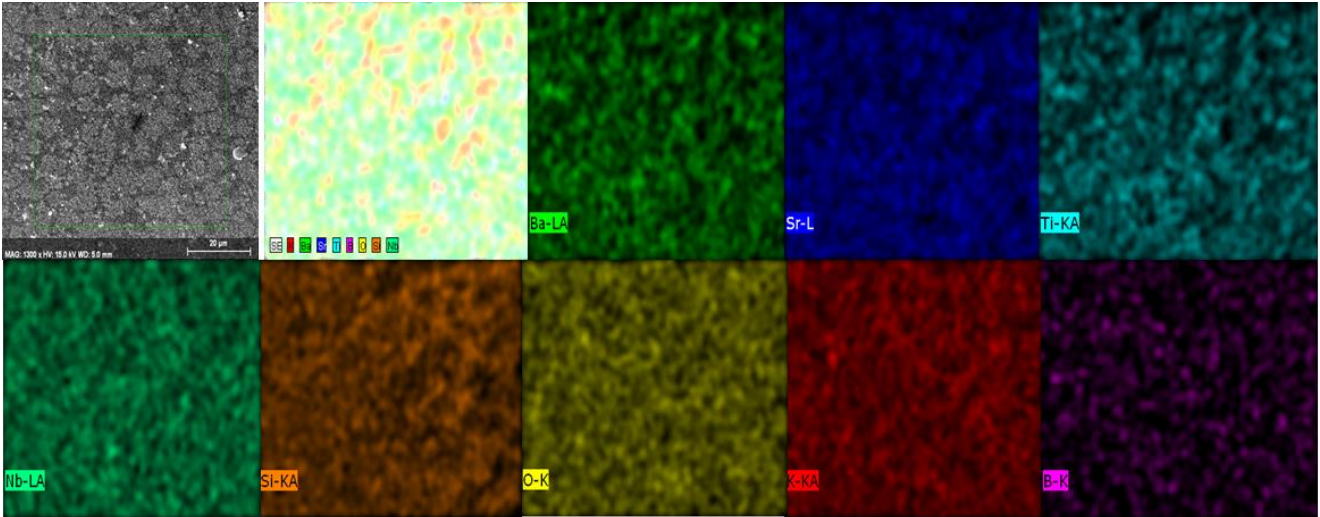


**Fig. 22** Elemental X-ray mapping showing the distributioun of elements for 0.1 mol % doped  $\text{Nb}_2\text{O}_5$  SBT glass ceramic

## 4.7 DIELECTRIC ANALYSIS

### MEASUREMENT AT ROOM TEMPERATURE WITH VARYING FREQUECNY

The dielectric constant ( $\epsilon$ ) as well as the dissipation factor ( $\tan \delta$  or  $D$ ) for both the glass samples were measured using the HIOKI LCR meter. First the SBT base glass having the composition  $[(\text{Ba}_{0.2}\text{Sr}_{0.8})\text{O}.\text{TiO}_2]-[2\text{SiO}_2-\text{B}_2\text{O}_3]-[\text{K}_2\text{O}]$  and second the 0.1 mol. %  $\text{Nb}_2\text{O}_5$  doped SBT glass ceramics having the composition  $[(\text{Ba}_{0.2}\text{Sr}_{0.8})\text{O}.\text{TiO}_2]-[2\text{SiO}_2-\text{B}_2\text{O}_3]-[\text{K}_2\text{O}]-0.1[\text{Nb}_2\text{O}_5]$ . For the above two samples dielectric measurement were done at room temperature with varying frequency. In case of the first sample  $[(\text{Ba}_{0.2}\text{Sr}_{0.8}).\text{O}.\text{TiO}_2]-[2\text{SiO}_2-\text{B}_2\text{O}_3]-[\text{K}_2\text{O}]$  it was observed that the dielectric constant ( $\epsilon$ ) measured at room temperature remains constant ( $\sim 18$ ) over the wide range of measured frequencies 100Hz, 1 kHz, 10 kHz, and 1000 kHz and 1 MHz, on the other hand dielectric loss or dissipation factor ( $\tan \delta$  or  $D$ ) for this sample is found to be very low i.e.  $< 0.01$ . But at low frequencies this value for ( $\tan \delta$  or  $D$ ) is  $\sim 0.04$ , which can be very well observed from the **Fig. 23**. In the case of the second sample 0.1 mol. %  $\text{Nb}_2\text{O}_5$  doped SBT glass ceramics having the composition  $[(\text{Ba}_{0.2}\text{Sr}_{0.8})\text{O}.\text{TiO}_2]-[2\text{SiO}_2-\text{B}_2\text{O}_3]-[\text{K}_2\text{O}]-0.1\text{mol \% } [\text{Nb}_2\text{O}_5]$ , it was observed that the dielectric constant ( $\epsilon$ ) remains constant ( $\sim 26$ ) over the wide range of measured frequencies 100Hz, 1 kHz, 10 kHz, and 1000

kHz and 1 MHz, on the other hand dielectric loss or dissipation factor ( $\tan \delta$  or D) for this sample is found to be very low i.e.  $<0.01$ . But at low frequencies this value for ( $\tan \delta$  or D) is in the range (0.04-0.08), which can be very well observed from the **Fig. 24**. Hence we can say that due to the doping of 0.1 mol. %  $\text{Nb}_2\text{O}_5$  there is a minor change in the dielectric constant.

#### MEASUREMENT AT ELEVATED TEMPERATURE WITH VARYING FREQUENCY

The dielectric constant ( $\epsilon$ ) as well as the dissipation factor ( $\tan \delta$  or D) for both of the glass samples were measured with temperature. For the glass ceramic samples dielectric measurement were done at elevated temperature with varying frequency. In case of the SBT base glass ceramic sample having the composition  $[(\text{Ba}_{0.2}\text{Sr}_{0.8})\cdot\text{O}\cdot\text{TiO}_2]\text{-}[\text{2SiO}_2\text{-B}_2\text{O}_3]\text{-}[\text{K}_2\text{O}]$ , it was observed that the at low frequency for 100Hz, 1kHz the dielectric constant remains constant up to 400K but then after it starts increasing, whereas in case of high frequencies 10 kHz, 100kHz, 1MHz the dielectric constant remains constant in the range of (37-42). That can very well be observed from the **Fig. 25**. On the other hand the dissipation factor at low frequency 100Hz, 1 kHz was seen to remain constant up to 400K but thereafter it starts to increase, whereas in case of high frequencies 10 kHz, 100 kHz, 1 MHz the dissipation factor remains constant  $<0.01$ , irrespective of the temperature change from 300 to 500K. as can be observed from the **Fig. 26**. In case of the second sample 0.1 mol. %  $\text{Nb}_2\text{O}_5$  doped SBT glass ceramics having the composition  $[(\text{Ba}_{0.2}\text{Sr}_{0.8})\cdot\text{O}\cdot\text{TiO}_2]\text{-}[\text{2SiO}_2\text{-B}_2\text{O}_3]\text{-}[\text{K}_2\text{O}]\text{-}0.1[\text{Nb}_2\text{O}_5]$ , it was observed that the at low frequency for 100Hz, 1 kHz the dielectric constant is in the range of 40-50 at temperature around 300K but with increasing temperature from 300K to 350K the dielectric constant value is found to be decreasing up to 35 and thereafter it remains constant up to 450K irrespective of frequency, then again after 450K the dielectric constant is found to be increasing for low frequencies 100Hz, 1 kHz, which can be very well observed from the **Fig. 27**. On the other hand, it was seen that the at low frequency 100Hz, 1 kHz the dissipation factor is in the range of 0.2-0.3 at temperature around 300K but on increasing temperature from

300K to 400K the dissipation factor value is found to be decreasing up to  $<0.01$  and thereafter it remains constant up to 450K irrespective of frequency, thereafter from 450K the dielectric constant is found to be increasing for low frequencies 100Hz, 1kHz, which can be very well observed from the **Fig. 28**. Hence we can say that due to the doping of 0.1 mol. %  $\text{Nb}_2\text{O}_5$  we didn't find much difference in the dielectric constant but in comparison to the un-doped base glass ceramic where the dissipation factor was found to be increasing at low frequency 100Hz, 1 kHz, the doped glass ceramic is found to have a very low dissipation factor.

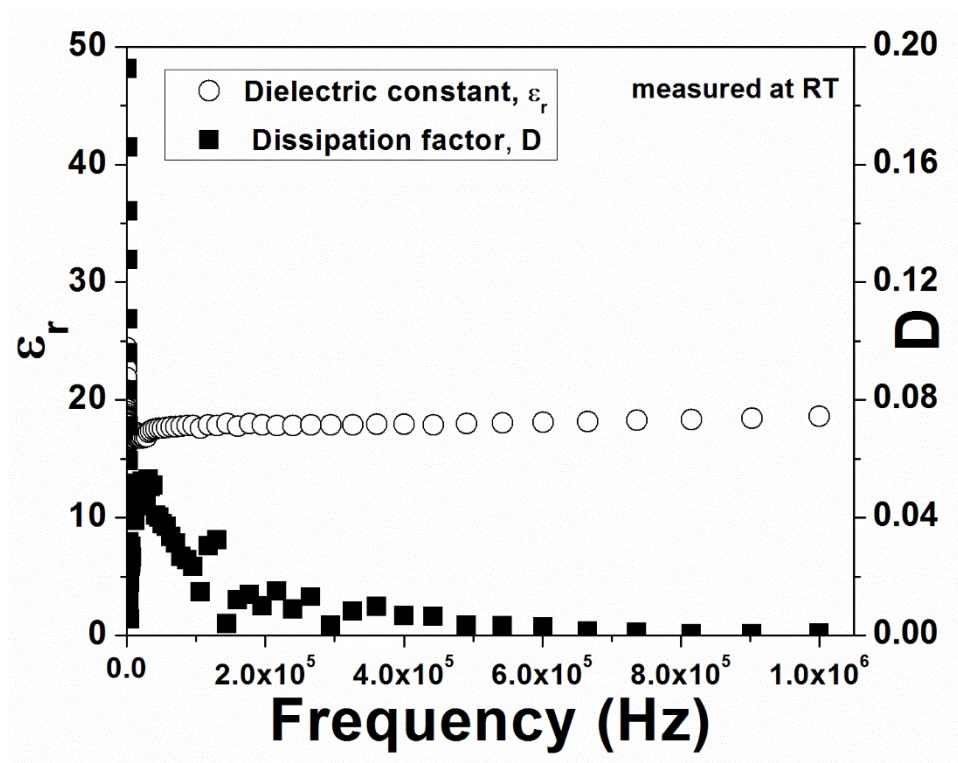


**Fig. 23** Dielectric measurement of SBT base glass ceramics at room temperature

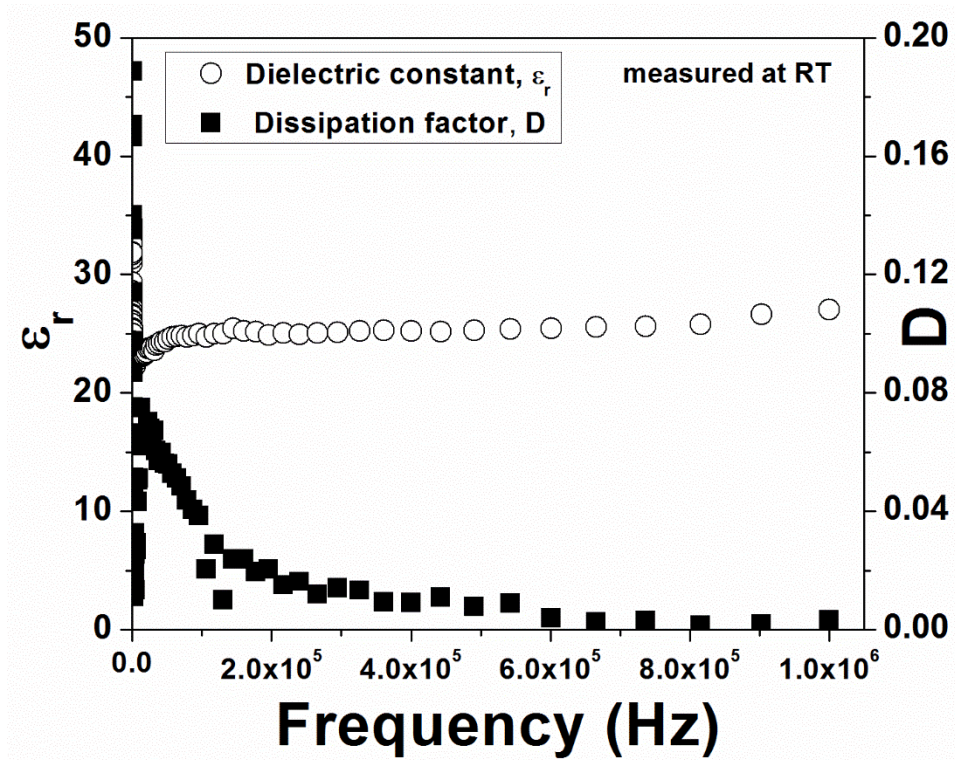


**Fig. 24** Dielectric measurement of doped glass ceramics at room temperature

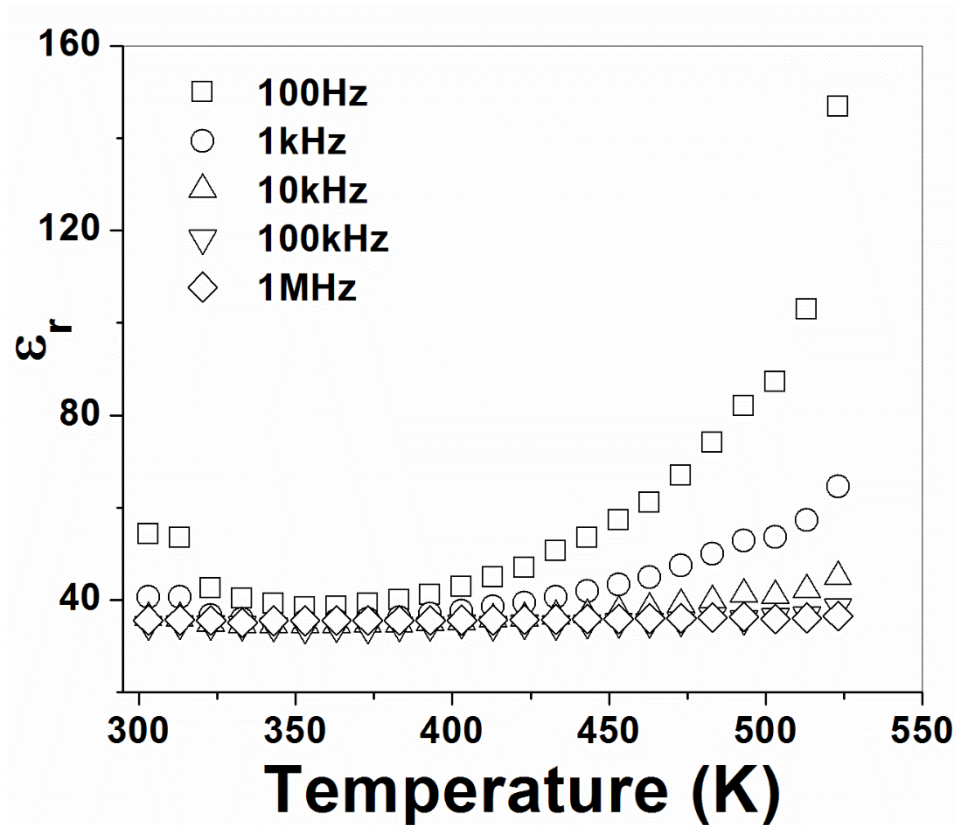


**Fig. 25** Measurement of dielectric constant with varying temperature for SBT base glass ceramic

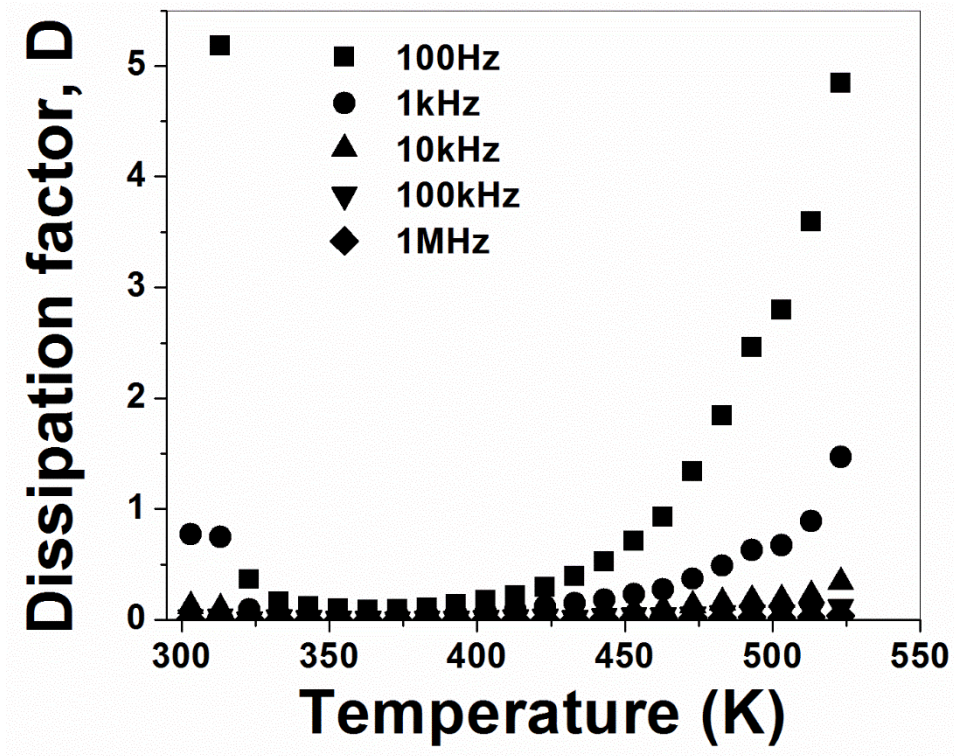


**Fig. 26** Measurement of dissipation factor with varying temperature for SBT base glass ceramic

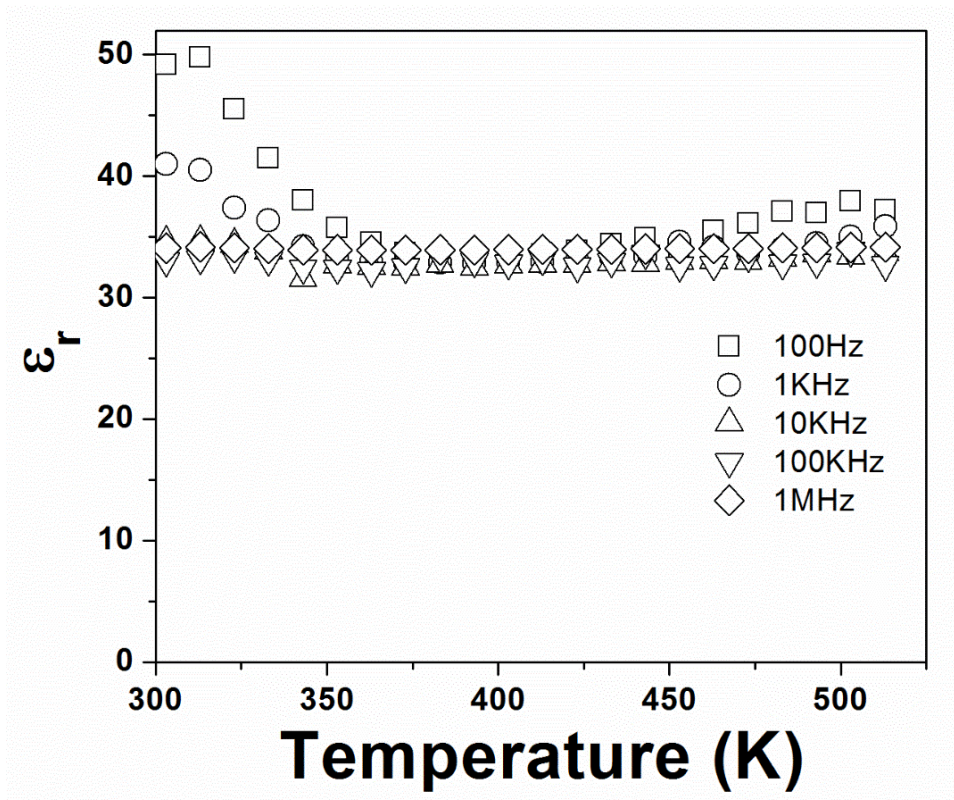


**Fig. 27** Measurement of dielectric constant with varying temperature for 0.1 mol %  $\text{Nb}_2\text{O}_5$  doped SBT glass ceramic



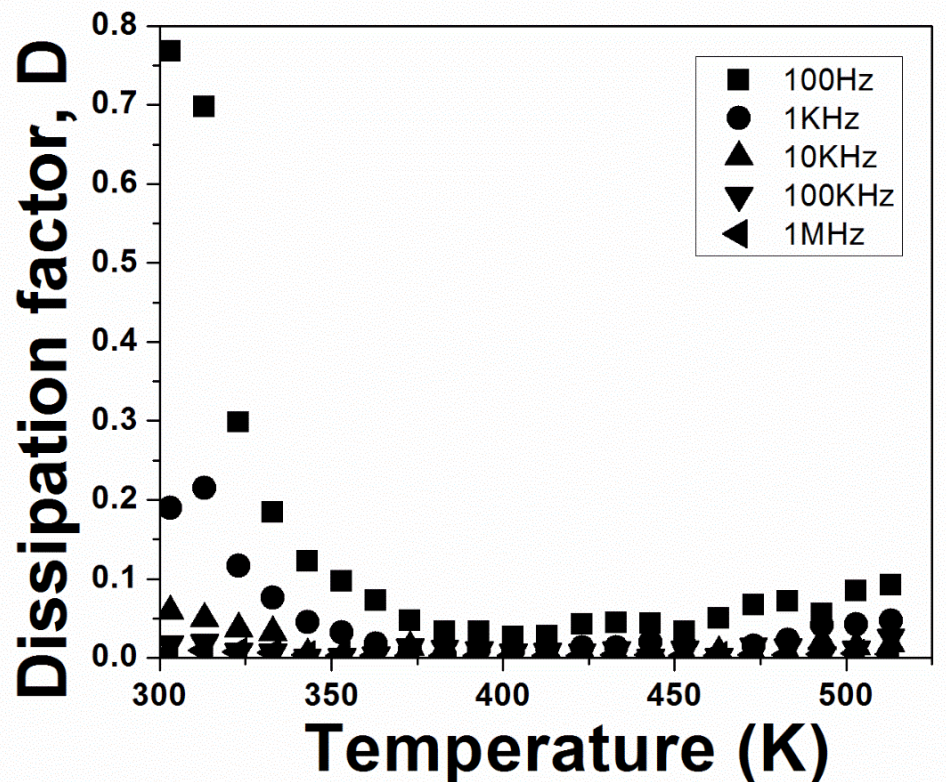


**Fig. 28** Measurement of dissipation factor with varying temperature for 0.1 mol % Nb<sub>2</sub>O<sub>5</sub> doped SBT glass ceramic

## CONCLUSION

The glass samples with and without doping of 0.1 mol. % Nb<sub>2</sub>O<sub>5</sub> were prepared successfully in the SBT borosilicate glass system. FTIR studies reveals that both the undoped and doped glass samples have different bonding modes such as transmittance peak due to stretching of O-H bond inside the glassy network, hydrogen bonding in the glassy matrix, bending of diborate (B-O-B) linkages, vibrational mode of the borate network, stretching vibration of the B-O-Si linkages, vibration of metal cation (Ba<sup>2+</sup>, Sr<sup>2+</sup>). Density measurement for both glass as well as glass ceramic samples were done using Archimedes principles and it was observed that there is a slight increase in the density of the glass ceramic as compared to the base glass. From the XRD analysis it was confirmed that the desired SrBaTiO<sub>3</sub> has been formed after heat treatment at 780°C for 3hr in case of base glass whereas in the case of the doped glass the desired SrBaTiO<sub>3</sub> phase was achieved at 750°C for 3hr. Hence, it was

concluded that the addition of 0.1 mol% Nb<sub>2</sub>O<sub>5</sub> promotes the crystallization temperature at lower temperature, thus Nb<sub>2</sub>O<sub>5</sub> acts as a nucleating agent. SEM analysis for un-doped glass ceramic samples reveals the formation of dendritic, flower-like, and needle like crystals throughout the microstructure whereas addition of 0.1 mol% Nb<sub>2</sub>O<sub>5</sub> completely modifies the microstructure to irregular shaped crystals. Dielectric measurement for both un-doped and doped glass ceramic samples performed at elevated temperature with varying frequency didn't show any marked difference in the dielectric constant as well as the dissipation factor.

## REFERENCES

1. A. K. Yadav and C. R. Gautam, 'A review on crystallization behaviour of perovskite glass ceramics', *Advances in Applied Ceramics*, Vol 113 no 4 2014.
2. A K Yadav, C. R. Gautam, and Prabhakar Singh, 'Dielectric behaviour of lanthanum added barium strontium titanate borosilicate glass ceramic', *J Mater Sci: Mater Electron* DOI 10.1007/s10854-015-3013-4.
3. W. Li, Z. J. Xu, R. Q. Chu, and P. Fu, "Structure and Dielectric Behavior of La-Doped BaTiO<sub>3</sub> Ceramics", *Advanced Materials Research*, Vols. 105-106, pp. 252-254, Apr. 2010
4. X. Wang, Yong Zhang, Ivan Baturin, and Tongxiang Liang, 'Blocking effect of crystal-glass interface in lanthanum doped barium strontium titanate glass ceramics', *Materials Research Bulletin*, 48 (2013).
5. J. Wang, Xi Yao, Liangying Zhang, 'Preparation and dielectric properties of barium strontium titanate glass ceramics sintered from sol-gel derived powders', *Ceramics International*, 30 (2004).
6. S. Lahiry, and A. Mansingh, 'Dielectric properties of sol-gel derived barium strontium titanate thin films', *Thin Solid Films*, 516 (2008).
7. Ting Wu, Yongping Pu, and Pan Gao, 'Influence of Sr/Ba ratio on the energy storage properties and dielectric relaxation behaviours of strontium barium titanate ceramics', *J Mater Sci: Mater Electron*, (2013) 24:4105–4112.
8. G.H. Jaffari, M. Asad Iqbal, S.K. Hasanain, Awais Ali, and A.S. Bhatti, 'Effect of densification on the ferroelectric response of Ba<sub>0.4</sub>Sr<sub>0.6</sub>TiO<sub>3</sub>', *Solid State Communications*, 205 (2015), p-46–50.
9. A K Yadav, C. R. Gautam, and Prabhakar Singh, "Crystallization and dielectric properties of Fe<sub>2</sub>O<sub>3</sub> doped barium strontium titanate borosilicate glass", *RSC advances*, 2015.

10. S. Hasimoto, L. Kindermann, P. H. Larsen, F. W. Poulsen, and M. Mogensen, 'Conductivity and expansion at high temperature in  $\text{Sr}_{0.7}\text{La}_{0.3}\text{TiO}_{3-x}$  prepared under reducing atmosphere', *J Electroceram*, (2006) 16: 103–107.
11. Peter Blenow, Anke Hagen, Kent K. Hansen, L. Reine Wallenberg, and Mogens Mogensen, 'Defect and electrical transport properties of Nb-doped  $\text{SrTiO}_3$ ', *Solid State Ionics*, 179, (2008).
12. J. Karezewski, B. Riegel, M. Gazda, P. Jasinski, and B. Kusz, 'Electrical and structural properties of Nb-doped  $\text{SrTiO}_3$  ceramics', *J Electroceram*, (2010) 24:326–330.
13. C. R. Gautam, D. Kumar, and O. Prakash, 'IR study of Pb-Sr titanate borosilicate glasses', *Bull Mater Sci*, Vol. 33, No. 2, April 2010.
14. C. R. Gautam, A.K. Yadav, V.K. Mishra, and K. Vikram, 'Synthesis, IR and Raman Spectroscopic Studies of  $(\text{Ba,Sr})\text{TiO}_3$  Borosilicate glasses with addition of  $\text{La}_2\text{O}_3$ ', *Inorganic Non-metallic materials*, 2012.